Evolution of Quaternary Tholeiitic Basalt Eruptive Centers on the Eastern Snake River Plain, Idaho

Scott S. Hughes,[1] Paul H. Wetmore,[2] and Jason L. Casper[1]

ABSTRACT

The tectonic and magmatic evolution of Quaternary olivine tholeiites in the eastern Snake River Plain (SRP) are evaluated by their spatial distribution and geochemical signatures. Individual lava-flow groups and their associated shield-building eruptive centers are either exposed at the surface or inferred to exist beneath overlying volcanic layers. Stratigraphy and dimensions of overlapping subsurface flow groups rely heavily on current well and core-hole correlations interpreted from natural gamma logs of numerous wells in conjunction with petrographic, paleomagnetic, geochemical, and radiometric age investigations. Magmatic sources inferred from vent distribution are dispersed over a wide expanse of the subcontinental mantle beneath the eastern SRP. Major and trace element variations depict at least four general types of sources, although each flow group has a distinct chemical signature representing a separate zone of melting. Basaltic shield dimensions, geochemical signatures, and Sr-Nd isotopic analyses support magma genesis characterized by low-volume batches of melt extracted from local reservoirs within EM2-like upper mantle. The source region was variably enriched in incompatible elements, and perhaps compositionally stratified, by previous subduction and within-plate processes. The wide variation of trace elements observed within some flow groups suggests that, for each monogenetic shield volcano, either (1) a heterogeneous batch of magma is derived by variable low degrees of partial melting and erupted with minimal fractionation, or (2) magma is generated as a homogeneous batch, which undergoes extensive fractionation during successive pulses of eruption. Other scenarios cannot be ruled out entirely.

A comparison of the locations of inferred subsurface (buried) eruptive centers for the basaltic shields with the documented volcanic rift zones suggests that the zones must be either expanded to include the subsurface eruptive centers or broken into numerous smaller, inferred rift zones. This comparison requires that the zone in which strain is accommodated is more diffuse than inferred by previous studies. Extensional stress is not being mitigated within very narrow zones but rather is being distributed throughout a zone that may be as wide as 15 or 20 km. Rift systems probably occur over zones of partial melting that tend to migrate with time depending on ambient conditions and the availability of recently melted lithosphere. Regional tectonic extension allows a diminished component of compressive stress parallel to the eastern SRP axis, thus enabling rift zones to be oriented roughly parallel to Basin and Range faults.

Key words: tholeiitic basalt, eruptive centers, mafic magmatism

INTRODUCTION

The eastern Snake River Plain (SRP), an east-northeast-trending, 400-km-long, 100-km-wide topographic and volcanic depression, extends from Twin Falls to Ashton in southeastern Idaho. The terrain is mostly semiarid steppe developed on eolian and lacustrine soils that variably cover broad expanses of basaltic lava. Mountains and valleys associated with the Basin and Range Province bound the depression on the north and south

Editors' note: The manuscript was submitted in June 1998 and has been revised at the authors' discretion.

[1]Department of Geosciences, Idaho State University, Pocatello, ID 83209
[2]Department of Earth Sciences, University of Southern California, Los Angeles, CA 90089-0740

Hughes, S.S., P.H. Wetmore, and J.L. Casper, 2002, Evolution of Quaternary tholeiitic basalt eruptive centers on the eastern Snake River Plain, Idaho, *in* Bill Bonnichsen, C.M. White, and Michael McCurry, eds., Tectonic and Magmatic Evolution of the Snake River Plain Volcanic Province: Idaho Geological Survey Bulletin 30, p. 00?-00?.

and trend perpendicular to the eastern SRP axis. Quaternary basaltic volcanic rocks, eolian sand, loess, and alluvial and lacustrine sediments were deposited on Miocene-Pliocene rhyolitic ash-flow tuffs now exposed only in ranges along the margins of the plain. Monogenetic basaltic shield volcanoes dominate the physiography of the eastern SRP (Figure 1) and the upper 1-2 km of the crust (Kuntz and others, 1992). Basaltic lava flows make up most of the stratigraphy, although other important Quaternary volcanic features include rhyolitic domes, phreatomagmatic volcanoes, and polygenetic eruptive centers composed of pyroclastic cones and chemically evolved lavas.

Geologic maps by Kuntz (1979), Scott (1982), and Kuntz and others (1988, 1994) and investigations into mechanisms of eastern SRP basaltic volcanism by Prinz (1970), Greeley and King (1977), Greeley (1982), Kuntz (1992), and Kuntz and others (1982, 1986, 1992) indicate a preponderance of fissure-erupted lavas that produce small coalescent shield volcanoes, each of which has grown over short periods of months or years. Holocene examples include the Wapi and Hells Half Acre

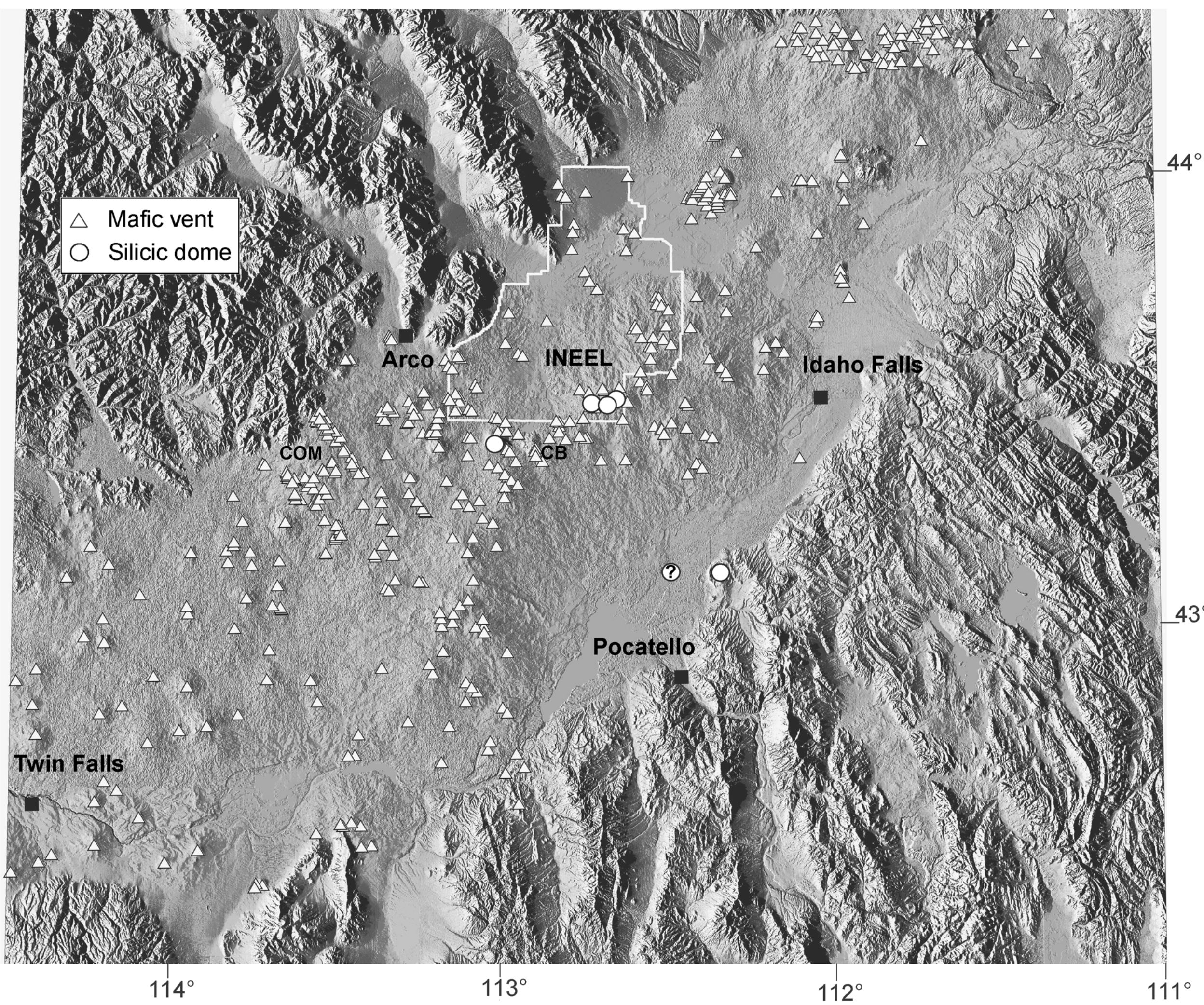

Figure 1. Shaded digital elevation model (DEM) composite map of the eastern SRP showing locations of Quaternary mafic eruptive centers (triangles) and silicic domes (circles). Eruptive centers were obtained from geologic maps of LaPoint (1977), Kuntz and others (1988, 1994) and topographic map interpretations and field investigations by the authors. Several vent clusters, such as those northwest of Idaho Falls, are probably rootless vents over a system of lava tubes from Table Butte, not individual shields. The linear array of vents southwest of Arco represents the latest Pleistocene-Holocene eruptions along the Great Rift. Abbreviations: COM—Craters of the Moon volcanic field, CB—Circular Butte (both of which are compositionally evolved centers), and INEEL—Idaho National Engineering and Environmental Laboratory boundary.

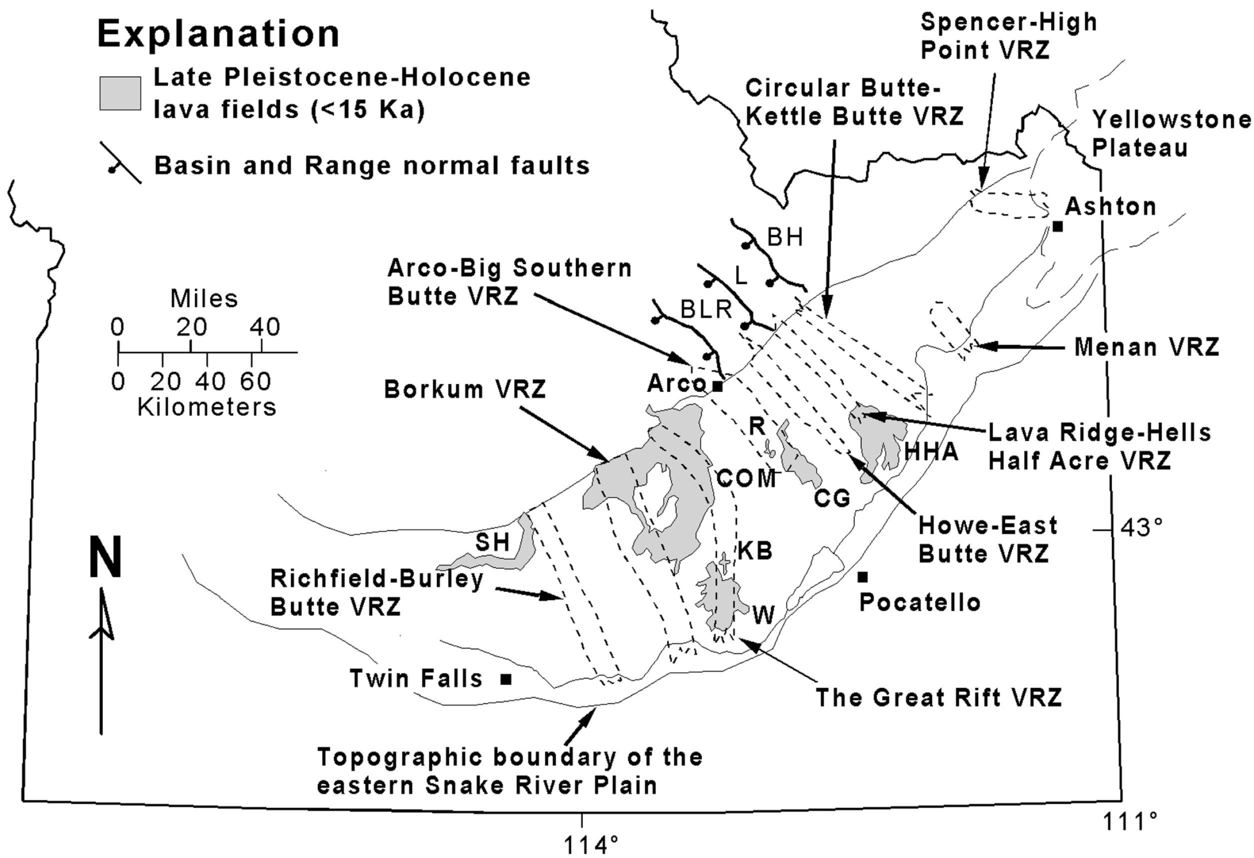

Figure 2. Map of eastern SRP illustrating the relations between volcanic rift zones (VRZs) proposed by Kuntz and others (1992), the location of Basin and Range normal faults northwest of the plain, and the latest Pleistocene-Holocene volcanic fields. Abbreviations for the volcanic fields: SH—Shoshone, COM—Craters of the Moon, KB—Kings Bowl, W—Wapi, R—North and South Robbers, CG—Cerro Grande, HHA—Hells Half Acre. Abbreviations for faults: BLR—Big Lost River, L—Lemhi, BH—Beaverhead.

lava fields (Figure 2), which are fairly uniform chemically and lithologically. Petrologic studies (Leeman, 1982b; Leeman and others, 1976) show that SRP basaltic lavas are dominantly diktytaxitic olivine tholeiites having either mildly enriched and fractionated chemical compositions (Group I) or somewhat primitive compositions with more affinity to magmatic sources (Group II).

Olivine tholeiites are chemically and petrologically distinct from evolved latitic compositions represented by Craters of the Moon (Leeman, 1982c; Kuntz and others, 1982, 1986, 1992), Cedar Butte (Hayden, 1992; Hayden and others, 1992; McCurry and others, 1999), and other locations that have experienced magmatic contamination, hybridization, or extensive fractionation. In contrast to magmatism at evolved centers where eruptions may occur intermittently over several thousand years (Kuntz and others, 1992), monogenetic eruptions represent small batches of magma that ascend from subcrustal sources without appreciable crustal residence time or interaction with crustal components (Leeman, 1982b; Kuntz, 1992).

The spatial distribution and major and trace element geochemical signatures of inferred subsurface eruptive centers (i.e., those that have been buried by younger volcanic or sedimentary deposits) are used in this paper to evaluate the tectonic and magmatic development of the eastern SRP mafic volcanic system. Chemical data were compiled from the literature and an extensive database (Hughes and others, 2000) of major and trace element whole rock analyses by ICP-AES and INAA of core-hole samples obtained in and around the Idaho National Engineering and Environmental Laboratory (INEEL). Stratigraphic and dimensional relations of lava flow groups at the INEEL rely on well and core-hole correlations, summarized by Anderson and others (1996), interpreted from natural gamma logs of numerous wells in conjunction with petrographic, paleomagnetic, geochemical, and radiometric age investigations. Stratigraphic studies at the INEEL have greatly improved the knowledge of eastern

SRP volcanic evolution and are used extensively in the following discussions.

VOLCANIC STRATIGRAPHY

Widespread basaltic volcanism has occurred intermittently on the eastern SRP throughout Pleistocene and Holocene time, an observation that argues for a high probability of mafic volcanism recurring (Hackett and others, this volume). Many of the eastern SRP volcanic landforms and eruptive mechanisms were described as basaltic plains-style volcanism by Greeley (1977; 1982). Interspersed among shields are eruptive and noneruptive fissures, evolved eruptive centers with composite cones, rhyolite domes, and sedimentary interbeds (Figure 3). Basaltic shields are topographically elevated and control the deposition of younger sediments and lavas (e.g., Hughes and others, 1997a). Modern sediments are distributed on the eastern SRP largely in eolian sands, lacustrine (playa-like "sinks"), and fluvial depositional systems (Hackett and Smith, 1992; Kuntz and others, 1992, 1994; Geslin and others, 1997; Gianniny and others, 1997). Eruptive centers exposed on the surface in and around the INEEL and other parts of the eastern SRP range in age from about 1.2 Ma to about 2.1 Ka (Kuntz and others, 1992, 1994), and radiometric ($^{40}Ar/^{39}Ar$) ages for core-hole basalts are as old as 3.2 Ma (D. Champion, written commun., 1998). Hackett and others (this volume) present a more in-depth discussion of the physical volcanology and timing of volcanic events on the eastern SRP. See Welhan and others (this volume) for a detailed assessment of lava-flow morphology and emplacement mechanisms.

The complex volcanic and sedimentary stratigraphy in the eastern SRP (Hughes and others, 1998) is partially solved by the surface and subsurface (test wells and core holes) correlation of flow groups based on uniform physical and chemical properties: natural gamma emissions, paleomagnetic polarity and inclination, radiometric age, petrography, and chemical compositions (e.g., Champion and others, 1988, 1996; Anderson, 1991; Lanphere and others, 1994; Anderson and Bartholomay, 1995; Anderson and Bowers, 1995; Reed and others, 1997). However, the distinction between two or more widely spaced flow groups may not always be evident on the basis of available physical parameters, age relations, and chemical parameters. Thus, flow groups may be combined into a larger "supergroup" of lavas, as used by Welhan and others (1997; this volume) and Wetmore and others (1997), which are coeval in volcanic stratigraphy but represent multiple, essentially unrelated eruptive centers. Subsurface topographic and isopach maps, based on current stratigraphic interpretations of well data by Anderson and others (1996), indicate that many inferred subsurface flow groups are, in fact, supergroups comprising several flow groups erupted from two or more distinct shield volcanoes (Wetmore, 1998; Wetmore and others, 1997).

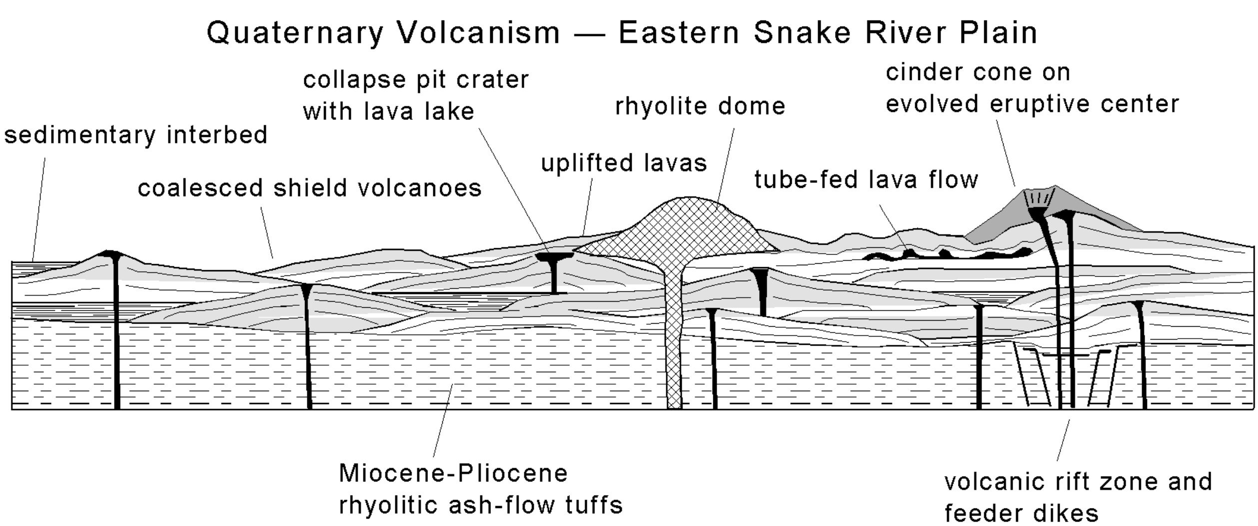

Figure 3. Schematic diagram of basaltic plains-style volcanism on the eastern SRP. Modified from Greeley (1977), the diagram illustrates myriad magmatic and surficial processes that contribute to the evolution of the province.

TECTONIC CONTROLS ON MAGMATISM

Late Tertiary tectonics in the northwestern U.S. produced a complex magmatic system. The currently accepted tectonic explanation for the eastern SRP and its extensions is that the province was formed above the track of the Yellowstone hot spot and possibly created by the passage of the North American plate southwestward over a stationary deep-seated mantle plume (Armstrong and others, 1975; Leeman, 1982a; Pierce and Morgan, 1992; Smith and Braile, 1994). Widespread mid-Miocene volcanism in eastern Oregon, northern Nevada, and southwestern Idaho lends support to the mantle plume hypothesis. Geist and Richards (1993) suggest that the relative volcanic ages and positions of SRP volcanics and the Columbia River basalts can be explained, in part, by the northward deflection of an ascending mantle plume about 20 Ma by the subducting Farallon plate. According to their model, the downgoing slab was subsequently penetrated about 17.5 Ma, and this allowed the plume to pass through to produce the Columbia River basalt and the Yellowstone hot-spot track. Camp (1995) proposes that the north-northwest alignment of mid-Miocene volcanism along the Nevada-Oregon rift zone resulted from compression and distortion of the plume head against the cratonic margin of North America between 17 Ma and 14 Ma. His model allows for a spread in volcanic activity away from the center of the plume and a southward shift in volcanism at about 14 Ma, as the distorted plume crest was overridden by Precambrian crust.

Although the mantle plume hypothesis is consistent with many features of eastern SRP magmatism, it does not account for some regional volcanic features, such as widespread Quaternary SRP volcanism that does not follow a time-transgressive trend and irregular time-space patterns of some major rhyolitic eruptions (e.g., see Hughes and McCurry, this volume). An added complication is the apparent southeast-to-northwest time-transgressive trend in Oregon volcanism that is the mirror image of the SRP trend (Luedke and Smith, 1982). These complications are partly explained by Saltzer and Humphreys (1997) who used seismic tomographic imaging to reveal a narrow, deep low-velocity region beneath, and parallel to, the eastern SRP. The low-velocity mantle corridor, composed of partially melted peridotite, is flanked by zones of high-velocity mantle that is probably depleted, relatively buoyant residual mantle from which SRP mafic magmas were derived. The residuum flattens and widens with distance from the hot spot and acts as a barrier that channels partial melts in the direction of plate motion (southwest) as the hot spot impinges on the craton. Thus, the tomographic model implies local convection controlled by partial melting and melt extraction, and it may help explain the presence of Quaternary volcanism on the eastern SRP subsequent to passage of the hot spot.

Basaltic lavas typically erupted from fissures along, and subparallel to, NW-SE volcanic rift zones that parallel Basin and Range structures. Volcanic rift zones (VRZs) on the eastern SRP (Figure 2) appear as linear sequences of basaltic vents and dikes with associated fissure-fed flows and open fissures generally parallel to, but not collinear with, range-front faults north and south of the plain (Kuntz and others, 1992). Tectonic SW-NE extension on the eastern SRP is possibly accommodated aseismically by dike injection and dilation (Rodgers and others, 1990; Parsons and Thompson, 1991; Hackett and Smith, 1992; Parsons and others, 1998) as opposed to normal faulting associated with Basin and Range extension. Kuntz and others (1992) and Hackett and Smith (1992) suggest that VRZs behave as offset extensions of the range-front faults in that they localize strain. Deformation in areas near eruptive centers includes linear fractures, grabens, and monoclines due to shallow magma injection. The orientation of inferred basaltic feeder dikes, as evidenced by the strong alignments of surface deformation features and vents, suggests that they reflect, at least in part, a regional SW-NE direction of either extensional stress or least-compressive stress.

The eastern SRP and immediately adjacent Basin and Range Province include the seismic collapse shadow of Anders and others (1989), which is an aseismic region surrounded by the seismically active part of the Basin and Range Province. No faults at the surface of the eastern SRP have significant (more than 10 m) offset; consequently, the means by which strain is partitioned between the collapse shadow and the seismically active Basin and Range Province have become debatable. Parsons and Thompson (1991) suggest that seismicity and topography are being suppressed by the dilation of dikes which feed the SRP lava fields. They argue that magmatic overpressure increases the magnitude of the least principle stress (3) and therefore decreases the magnitude of differential stress (1-3), which would otherwise be released in a faulting event. Parsons and others (1998) quantified the strain rate of the eastern SRP since 4.5 Ma and suggest that the eastern SRP has been extending at a rate consistent with that of the seismically active part of the Basin and Range Province. Conversely, Anders and Sleep (1992) conclude that mafic midcrustal intrusions, associated with the passage of the region over a mantle plume, act as a rigid body possessing sufficient strength to resist brittle failure. Their assertion is, therefore, that the eastern SRP is not significantly extending relative to the seismically active Basin and Range Province.

The surficial geometry of eruptive centers, dikes, fissures, and rift zones on the eastern SRP implies that regional stress has some effect on basaltic magma emplacement in reservoirs in the upper mantle or lower crust where primary melts accumulate above the region of partial melting. The magmatic model by Kuntz (1992) indicates basaltic magma stored beneath eastern SRP eruptive centers in narrow elongate sill and dike networks oriented perpendicular to the direction of least-compressive stress. Regional horizontal extension causes magmas to locally penetrate all levels of the lower and middle crust along vertical dikes. This model implies that eastern SRP extension-related magmatism is comparable to that measured or inferred at active basalt rift systems, although the mechanisms of extension may differ somewhat. Noneruptive fissures and grabens (Kuntz and others, 1988, 1994) extending beyond the edges of Holocene volcanic fields and away from their eruptive centers may be related to lateral dike propagation away from the eruptive part of the fissure as well as vertical dike propagation above the reservoir (Pollard and others, 1983; Rubin and Pollard, 1987; Rubin, 1992; Hackett and Smith, 1992). As a dike ascends into overlying basaltic layers, the extension above the advancing dike produces nested grabens (Figure 4), providing topographic lows where lava accumulates.

Dikes propagate when the stress at the dike tip exceeds the fracture toughness of the host rock (Rubin and Pollard, 1987). The stress intensity at the tip is influenced by dike geometry and the difference between magma pressure and the ambient stress, i.e., magmatic overpressure. Ambient stress cannot be isotropic during eastern SRP eruptions as evident in the NW-SE alignment of volcanic fissure systems. Another important factor in the style of eastern SRP magmatism, and its dependency on crustal extension, is a relatively low magmatic supply rate reflected in numerous small batches of magma that produce monogenetic eruptive centers (Figure 1) rather than large complex shields. Compared to regions of high eruption rates, such as Hawaii or Iceland where shield tumescence due to magma injection is followed by deflation during an eruption, eastern SRP magma reservoirs perhaps do not undergo significant readjustment during an eruption. The modeling of eastern SRP basalt magmatism by Kuntz (1992) suggests that a lack of immediate crustal response during an eruption results in low-volume, short-lived eruptions because a progressive pressure drop occurs as the reservoir is depleted. Eastern SRP eruptions terminate at a critical pressure level a relatively short time after the eruption begins. Thus, the extension rate is critically balanced with magma production.

The combination of low magma production rates and regional extension throughout the late Pliocene and Quaternary periods has resulted in the subsidence of the eastern SRP volcanic system. The overall subsidence of the eastern SRP relative to the Basin and Range Province was documented by McQuarrie and Rodgers (1998) in a study of structural attitudes of ranges with respect to distance from the SRP topographic depression. Their analysis indicates that the eastern SRP is a volcanic basin formed as a manifestation of crustal flexuring caused by isostatic readjustment due to an increase in midcrustal density. McQuarrie and Rodgers suggest that the midcrustal load is related to an inferred extensive mafic sill emplaced at approximately 10 Ma, which provided much of the heat for rhyolitic volcanism, and to the continual localized loads added by dikes and sills during Quaternary mafic volcanism. The subsidence rate apparently varies within the volcanic system. Differential subsidence is evident in volcanic-sedimentary stratigraphy and age relations of flow groups. Volcanic stratigraphy beneath the INEEL (Anderson and others, 1996; Reed

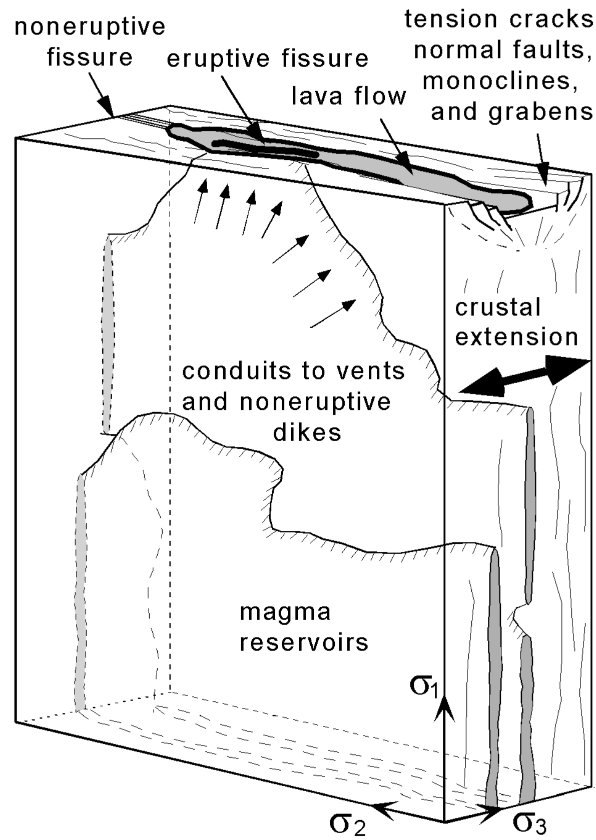

Figure 4. Schematic model of bladelike dike emplacement on the eastern SRP modified from Hughes and others (1997a). Lateral propagation is possible when the fracture toughness of the country rock is exceeded by magma pressure. Orientation of dikes are controlled by the regional stress field and vertical reservoirs probably become more like vertical blobs deeper in the crust (see Figure 16). The diagram is an adaptation of studies by Rubin and Pollard (1987), Kuntz (1992), and Hackett and Smith (1992).

and others, 1997; Hughes and others, 1997a; Wetmore, 1998) suggests that some eruptive centers have subsided significantly with respect to others; however, the relation between possible local subsidence and accommodating structures remains unclear.

DISTRIBUTION OF ERUPTIVE CENTERS

The distribution of eruptive centers reflects the existence and importance of volcanic rift zones (Kuntz and

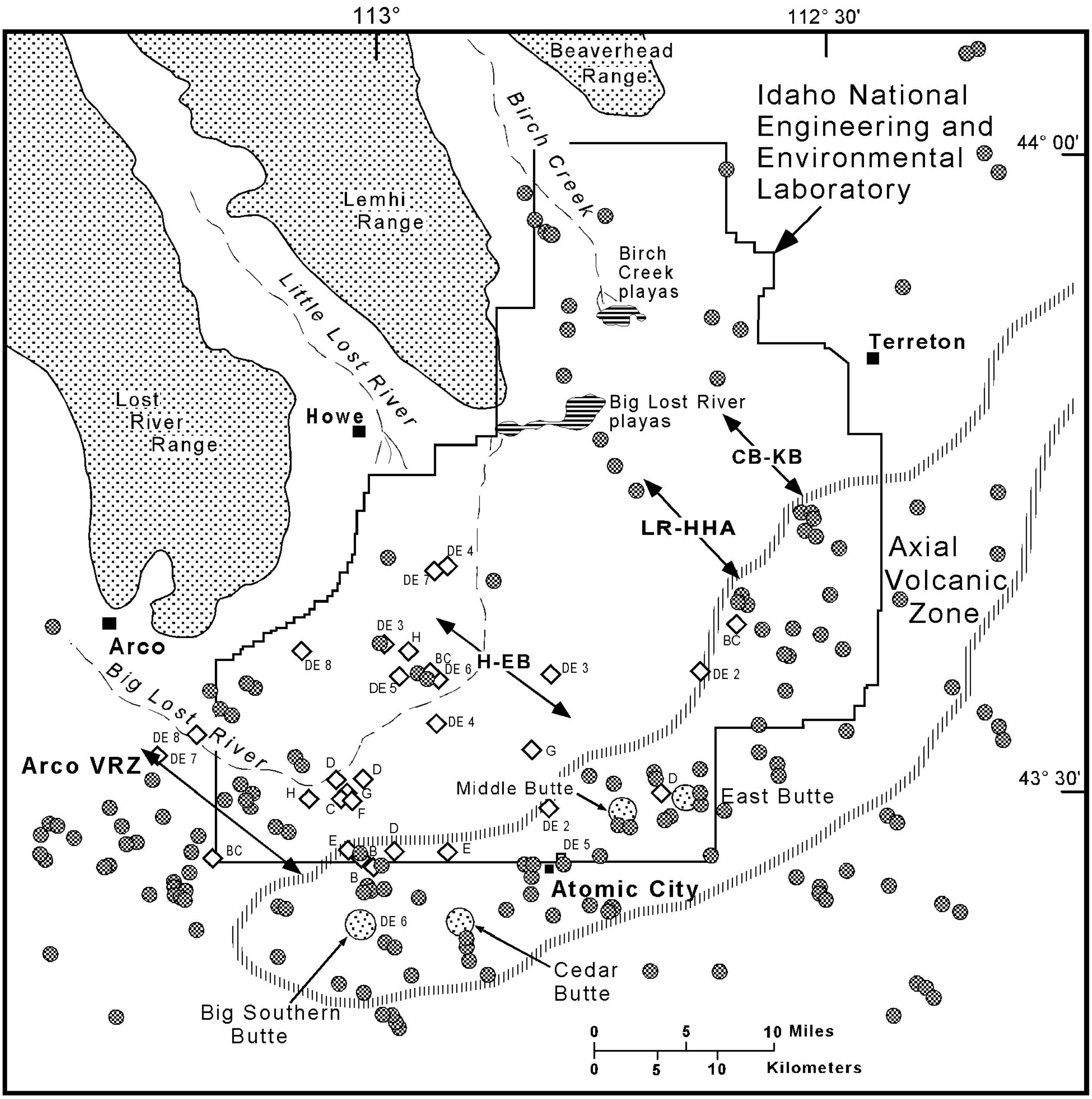

Figure 5. Map of the Idaho National Engineering and Environmental Laboratory region of the eastern SRP with locations of the axial volcanic zone relative to Quaternary volcanic vents exposed at the surface (filled circles) from Kuntz and others (1994) and inferred subsurface vents (diamonds) from Wetmore (1998). Arrows show the axes of volcanic rift zones shown by Kuntz and others (1992): Arco—Arco VRZ; H-EB—Howe-East Butte VRZ; LR-HHA—Lava Ridge-Hells Half Acre VRZ; and CB-KB—Circular Butte-Kettle Butte VRZ.

others, 1992) and can be used to evaluate localization and trends in the development of strain and magmatism (Wetmore, 1998; Anderson and others, 1999). During the past 200 k.y. basaltic volcanism in the central part of the eastern SRP has been concentrated along the northeast-trending axial volcanic zone (Figure 5), which constitutes the topographically high central axis of the eastern SRP (Hackett and Smith, 1992; Kuntz and others, 1992). Repose intervals ranged from 200 k.y. to 1,000 k.y. as evident in surface ages and sedimentary deposits. However, between about 200 Ka and about 600 Ka, the region in what is now the central and southern INEEL was volcanically active, producing as much as 58 cubic km of basalt per 100 k.y. (Wetmore, 1998).

The extensive interpretive stratigraphic database of flow groups and sedimentary interbeds provided by Anderson and others (1996) was used for spatial analysis of sixteen basalt supergroups representing the post-1 Ma time interval. Geochemical analyses and additional core logging since the Anderson and others' paper suggested only minor changes to their interpretations. Thus, the data were used to construct isopach maps of each supergroup (Wetmore and others, 1997) and to infer locations of their respective buried eruptive centers (Wetmore, 1998). These studies identified approximately thirty subsurface eruptive centers at and near the INEEL (Figure 5), most of which are associated with either a previously identified volcanic rift zone (VRZ), Arco-Big Southern Butte or Howe-East Butte, or the axial volcanic zone. Nearly all of the subsurface eruptive centers within the two VRZs lie in clusters so that they are within a few kilometers of each other. The number of middle-to-late Pleistocene eruptive centers in this region is due, in part, to the abundance of data in the southern part of the INEEL; however, surficial basalts and eruptive centers in the northern INEEL region typically are older than 800 k.y. (Kuntz and others, 1994).

Eruptive centers within the Arco-Big Southern Butte and Howe-East Butte VRZs have rough trends of decreasing age from the northwest to the southeast (supergroup and eruptive center ages increase from B to I). Eruptive centers for supergroups DE 8 and DE 7 are in the northwest, whereas supergroups DE 6, BC, and B are in the southeast. Similarly, within the Howe-East Butte VRZ supergroups, DE 7 and DE 4 eruptive centers are in the northwest; one of the supergroup DE 3 eruptive centers is to the southeast, and an eruptive center of supergroup D is still further southeast. Similar trends are apparent just west of the Howe-East Butte VRZ. Thus, volcanism at and near the INEEL appears to make a significant shift through time, producing hiatuses within areas of varied size and duration from 200 k.y. to nearly 1 m.y.

Volcanism between about 625 Ka and 200 Ka occurred in the southwestern and southeastern parts of the INEEL (Figure 6a-d); subsequent volcanism was in the axial volcanic zone (Figure 6e). Locally in the southwestern INEEL, volcanism appears to have shifted with time between the cluster of centers south of Big Lost River and the cluster on the north side of the river. The eruptive centers of supergroups I through F are concentrated within these two areas (Figure 6b). The eruptive centers of the two subsequent supergroups, DE 8 and DE 7, form a linear trend from south of Arco to southeast of Howe (Figure 6c). Eruptive centers of supergroup DE 6 through DE 2 are concentrated in the west-central INEEL north of the river and near Atomic City (Figure 6d). Eruptive centers within supergroup D through B are near the southern INEEL vent cluster, and a single eruptive center (BC) is in the cluster north of the river (Figure 6e). Since the emplacement of supergroup B, the volcanism has been within the axial volcanic zone (Figure 6f), and no eruptions since then have occurred within the INEEL.

GEOCHEMICAL AND LITHOLOGICAL IMPLICATIONS

The SRP volcanic system has been described as "bimodal" (rhyolite and basalt), but there are clearly intermediate compositions such as the evolved latitic rocks at Craters of the Moon and other eastern SRP locations (Leeman, 1982c; Kuntz and others, 1982, 1986, 1992; Honjo and Leeman, 1987; Stout and others, 1994) and latitic to rhyolitic associations at Cedar Butte (Hayden, 1992; Hayden and others, 1992; McCurry and others, 1999). Harker variation diagrams (Figure 7) illustrate well-defined alkalic and tholeiitic compositions based on the classification by Le Bas and others (1986). Chemical trends among the evolved alkalic compositions are clearly separated from the cluster of olivine tholeiites that erupted from monogenetic shields. Tholeiites range in SiO_2 from about 45 to 51 weight percent, whereas lavas in evolved eruptive centers range in SiO_2 from about 43 to 76 weight percent and have alkalic differentiation trends. Eastern SRP tholeiites have lower total alkalis ($Na_2O + K_2O$), higher MgO and CaO, and lower overall TiO_2 relative to Craters of the Moon lavas with equivalent SiO_2 values.

The coherence of major element trends in the evolved compositions implies a uniform process of magmatic evolution in the crust throughout the eastern SRP (Leeman, 1982c). Separation of the alkalic trend from the tholeiitic cluster possibly reflects markedly different magmatic sources; however, some tholeiitic compositions plot close to the alkalic Craters of the Moon trend. An

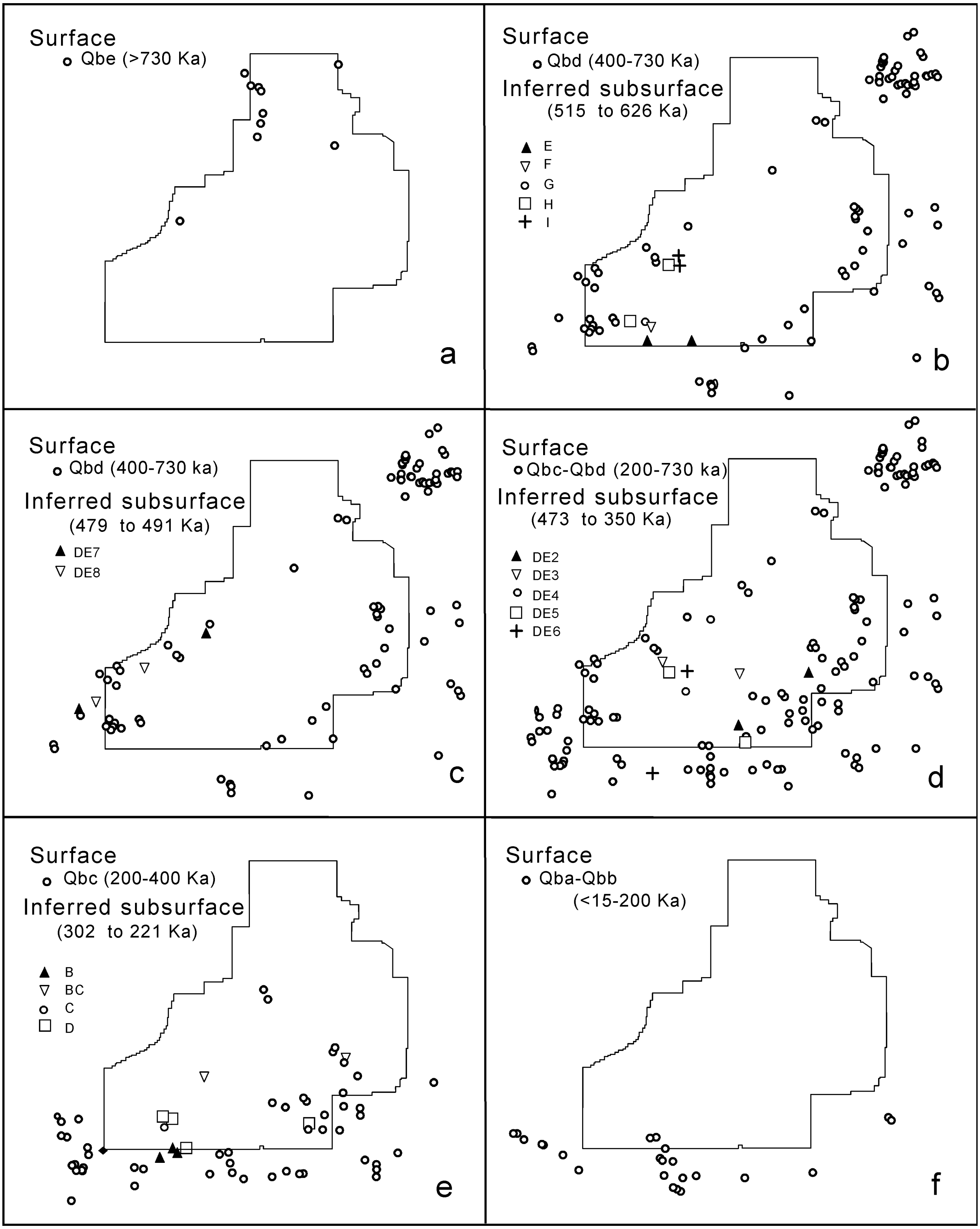

Figure 6. Time-sequential maps of surface and inferred subsurface volcanic centers near the INEEL (compare to Figure 5). Ages for eruptive centers Qba-Qbe are from Kuntz and others (1994); flow group (or supergroup) designations (B-I) are from Anderson and others (1996), and locations of inferred subsurface eruptive centers are from Wetmore (1998). The Qbd vent cluster northeast of the INEEL is probably a system of rootless vents on the flanks of Table Butte shield volcano, not individual shields.

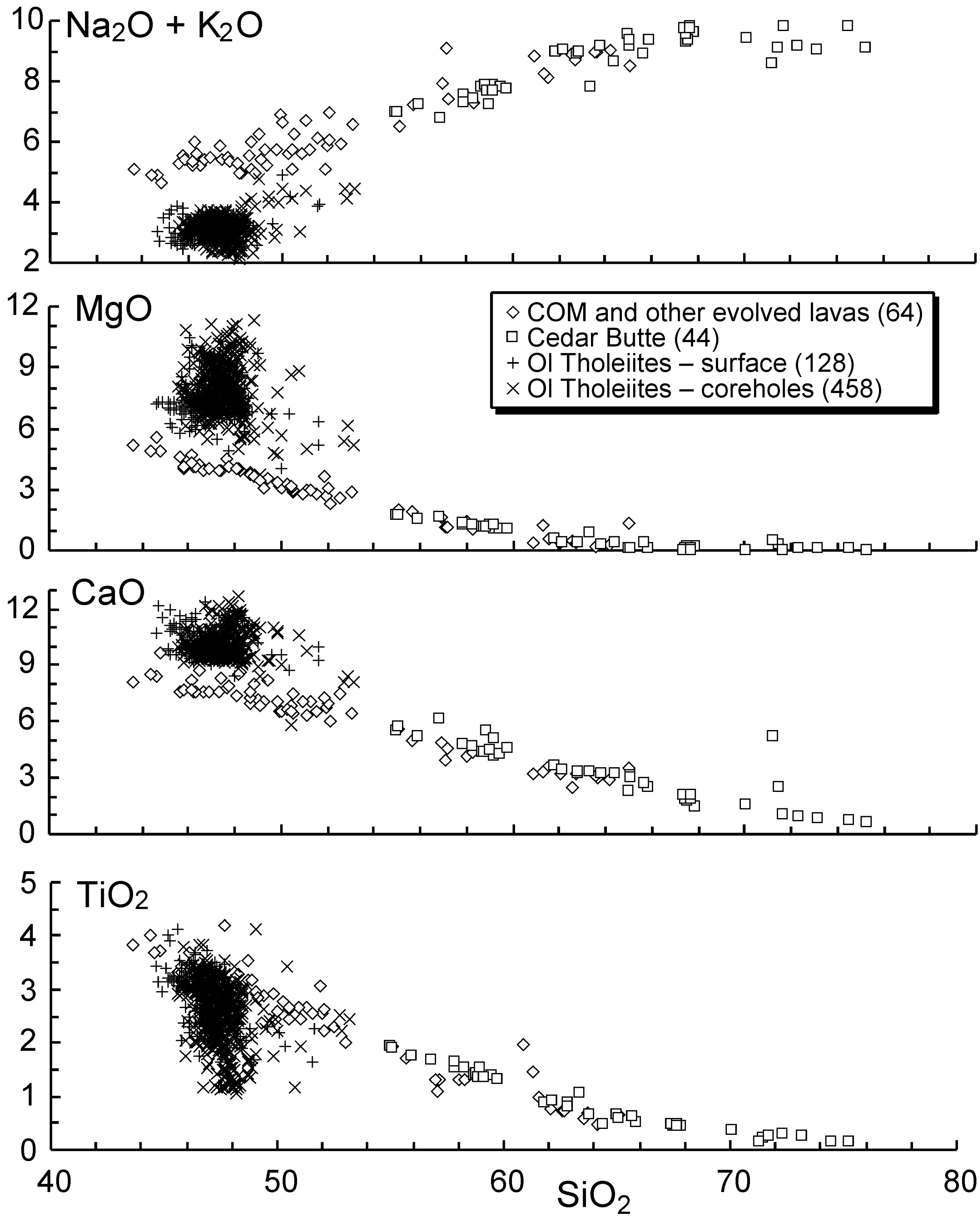

Figure 7. Harker diagrams of $Na_2O + K_2O$, MgO, CaO, and TiO_2 versus SiO_2 for eastern SRP olivine tholeiites, Craters of the Moon (COM), and Cedar Butte. Data sources: Hayden (1992); Knobel and others (1995); Kuntz and others (1985, 1992); Kuntz and Dalrymple (1979); Leeman (1982b, 1982c); Reed and others (1997); Shervais and others (1994); Stout and Nicholls (1977); and new analyses by the Idaho State University geochemical laboratory (Hughes and others, 2002).

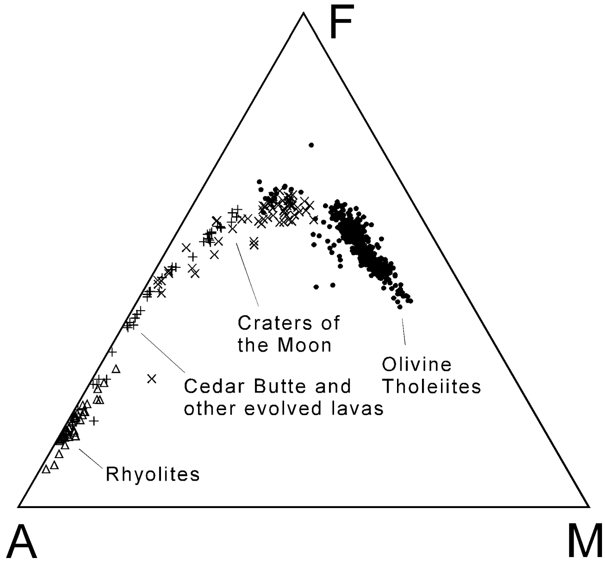

Figure 8. A-F-M diagram (A = $Na_2O + K_2O$, F = FeO, M = MgO — all in weight percent) of eastern SRP Quaternary volcanic rocks. Over 580 analyses are represented, with a few compositionally evolved exceptions, in the olivine tholeiite field. Data sources are the same as those listed in Figure 7.

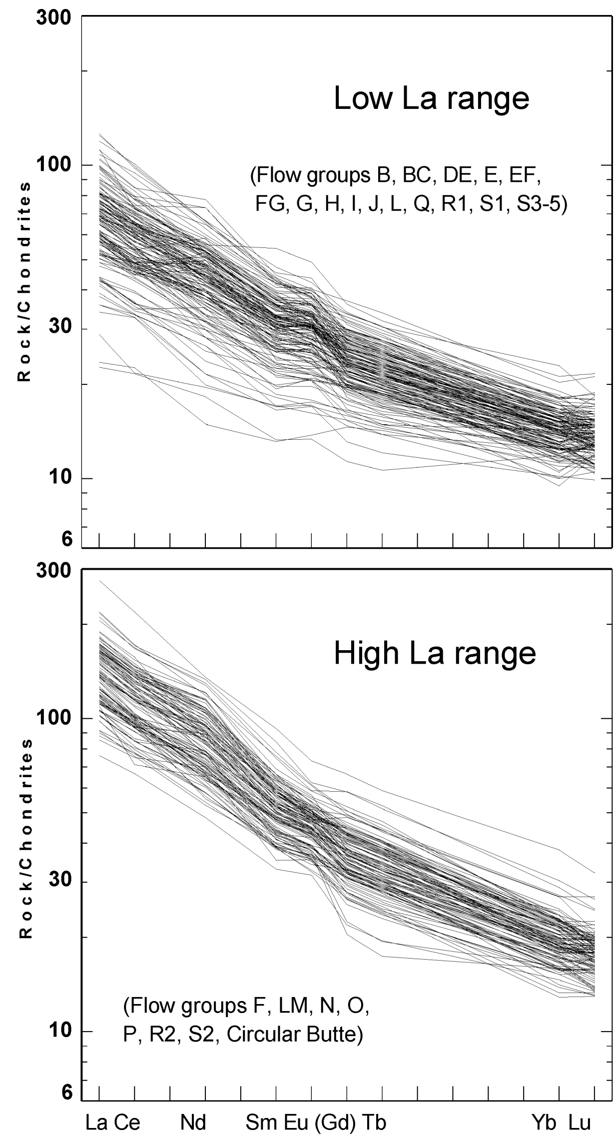

Figure 9. Rare earth element diagrams of tholeiitic basalt flow groups on the eastern SRP arbitrarily separated into compositional ranges with relatively low La (B, BC, DE, E, EF, FD, G, H, I, J, L, Q, R1, S1, S3, S4, and S5) and high La (F, LM, N, O, P, R2, S2, and Circular Butte). Except for Circular Butte lavas, flow group designations follow the terminology of Anderson and others (1996). Data are normalized to C1 chondritic abundances of Anders and Ebihara (1982) recalculated on a volatile-free basis.

AFM (Na_2O+K_2O – FeO – MgO) ternary diagram (Figure 8) shows a slight divergence away from the extremely tight cluster of most tholeiite analyses and a possible overlap with the trend observed in Craters of the Moon, Cedar Butte, and SRP rhyolites. This may simply reflect a relatively small amount of crustal evolution (contamination and fractionation) experienced by a few tholeiitic magmas representing the incipient stages of more extensive crustal interaction incurred by the evolved and hybrid compositions.

Chemical variation is significant within the tholeiitic basalts, although SiO_2 remains fairly constant compared to the evolved compositions. For example, TiO_2 ranges from about 1 to 4 weight percent, and MgO ranges from about 3.5 to about 12 weight percent, both of which have an overall 3-4X variation. Dispersion in other major oxides is also evident, although their overall ranges are not as dramatic. Substantial ranges in incompatible trace elements are exemplified in Figure 9 by rare earth element (REE) data normalized to C1 chondritic meteorites (Anders and Ebihara, 1982). Heavy REE (Yb and Lu) have an overall 3X range at 10-30 times chondrites, while light REE (La and Ce) have a nearly 10X overall variation at 22-200 times chondrites.

Compatibility with essential minerals in olivine tholeiites (olivine, plagioclase, pyroxene, and Fe-Ti oxides) increases with atomic number, so the ratio of light REE to heavy REE becomes fractionated during igneous processes. The REE patterns are plotted according to overall flow group chemistries (some are actually supergroups). Those with overall lower La ranges (B, BC, C, D, D3, DE4, DE6 to DE8, E, E1, EF, FG, G, G1, I, Q, R1, S1, S3-5, and Hells Half Acre) are plotted together in the upper part of Figure 9, and those with either relatively high La or a wide range of La (DE1, DE3, DE5, F, F1, LM1 to LM8, N, O , P, R2, S2, Wapi, Shoshone, Kings Bowl, N. Robbers, and S. Robbers) are plotted together in the lower diagram. Groups N, O, P, and Q, sampled in northern INEEL core holes, are slightly revised from the Anderson and Bowers (1995) and Anderson and others (1996) interpretations on the basis of recent geochemical data. Apparently, there is no relation between the REE signature and vent location in Figure 5. Distinction between the groups based on REE is rather arbitrary and admittedly includes overlapping compositional ranges, but the REE patterns show that some flow groups or supergroups vary widely in REE while others have more uniform REE abundances. Moreover, a gross difference in REE signature is apparent between two major groups of olivine tholeiites. Many additional analyses will be needed to refine this assessment and eliminate possible incorrect groupings.

Geochemical covariant plots of several elements and ratios (Figure 10) suggest that flow groups grossly cluster into separate covariant fields. Considerable overlap with adjacent groups and greater concentration ranges appear more in some components than in others. Individual low La groups have a greater variation in Cr, Sr, and MgO and lower overall Ba and La/Sm relative to the high La groups; high La groups have greater ranges in Sc and K_2O/TiO_2. Covariant trends are not readily defined, but many groups plot in loosely constrained fields that produce somewhat collinear patterns because each covariant plot represents elements that have similar but not equivalent chemical behaviors. Geochemical ranges of high La flow groups P and R2 are slightly more restricted compared with all other flow groups. Several groups, notably R1 and O, have elemental abundances that span the range between other groups. Perhaps all groups would have such high ranges with greater sampling density, but vertical chemical patterns in the INEEL cores (Shervais and others, 1994; Hughes and others, 1997c; Wetmore, 1998) reveal that some flow groups have systematic changes in geochemistry with distance above the base, whereas others are much more uniform throughout the entire thickness of the flow group.

PETROCHEMICAL PROCESSES

Geochemical and isotopic arguments (Leeman and others, 1976; Stout and Nichols, 1977; Leeman, 1982b; Menzies and others, 1984) support the petrogenesis of eastern SRP tholeiitic basalts by partial melting of fairly uniform spinel lherzolite, followed by the fractional crystallization of olivine and plagioclase, along with minor apatite and Fe-Ti spinels. Chemical trends observed in individual flow groups support magmatic fractionation during partial melting and crystallization; however, much of the overall chemical variation may represent local heterogeneity in source regions. This section summarizes the potential effects of these petrologic processes from the recent compilation of an extensive geochemical database and the evaluation of individual flow groups.

Chemical variation in lavas due to mineral-liquid-vapor phase separation is evident in the textures and mineral compositions of eastern SRP basalts. Local differences in phenocryst size and abundance, groundmass texture, and vesiculation may account for some heterogeneity. Eastern SRP basalts erupt as gas-charged magma that produces shelly pahoehoe lava near vents and gradually loses volatiles with distance to produce more massive lava flow interiors (Kuntz and others, 1994). Inspection of numerous flows in INEEL core reveals that many flow tops are highly vesiculated over a 2-4 m thickness, regardless of the total flow thickness, and that highly porous diktytaxitic textures prevail throughout most flow interiors. The petrography of INEEL core-hole and surface basalts by Kuntz (1980), Lanphere and others (1994), and this study reveals that most eastern SRP lavas are mineralogically similar and contain groundmass olivine, plagioclase, clinopyroxene, titanomagnetite, ilmenite, glass, and accessory apatite. Phenocrysts are olivine (0.5-3 mm), plagioclase (0.1-1 cm), and rare clinopyroxene. Textures are generally microporphyritic, glomerophyric, or diktytaxitic; grain size varies, and some coarsely diktytaxitic lavas contain plagioclase laths over 1 cm long. Textural differences in coarsely diktytaxitic lava are evident at outcrop scale and, in some places, at submeter scale where local unmixing of mineral and liquid phases produces bands of subphyric, fine-grained basalt within coarsely crystalline, porphyritic basalt (Hughes and others, 1999).

Microprobe analyses of dominant minerals in Circular Butte lavas (Figure 11) reveal compositional variation in olivine and plagioclases and uniformity in each of two populations of Fe-Ti oxides. Most phenocrysts are relatively unzoned, so olivine and plagioclase compositions tend to cluster near the Mg-rich and Ca-rich ends of their respective trends. The calculated olivine composition ($K_D = 0.3$, Fe-Mg fractionation) shown for Circular Butte lavas represents the initial composition expected during crystallization. The closeness of calculated initial and measured compositions and the lack of zoning suggest that phenocrysts crystallized under stable equilibrium conditions. The Fe-Ti oxide pairs have fixed compositions with the Fe-rich member approximately aligned with the overall trend of whole rock compositions.

The simple mass-balance evaluation of these mineral components (Shervais and others, 1994) shows that small amounts of olivine fractionation will produce significant overall variations in MgO and FeO. Likewise, plagioclase fractionation can account for CaO and Na_2O variations. Crystal fractionation effects would produce signifi-

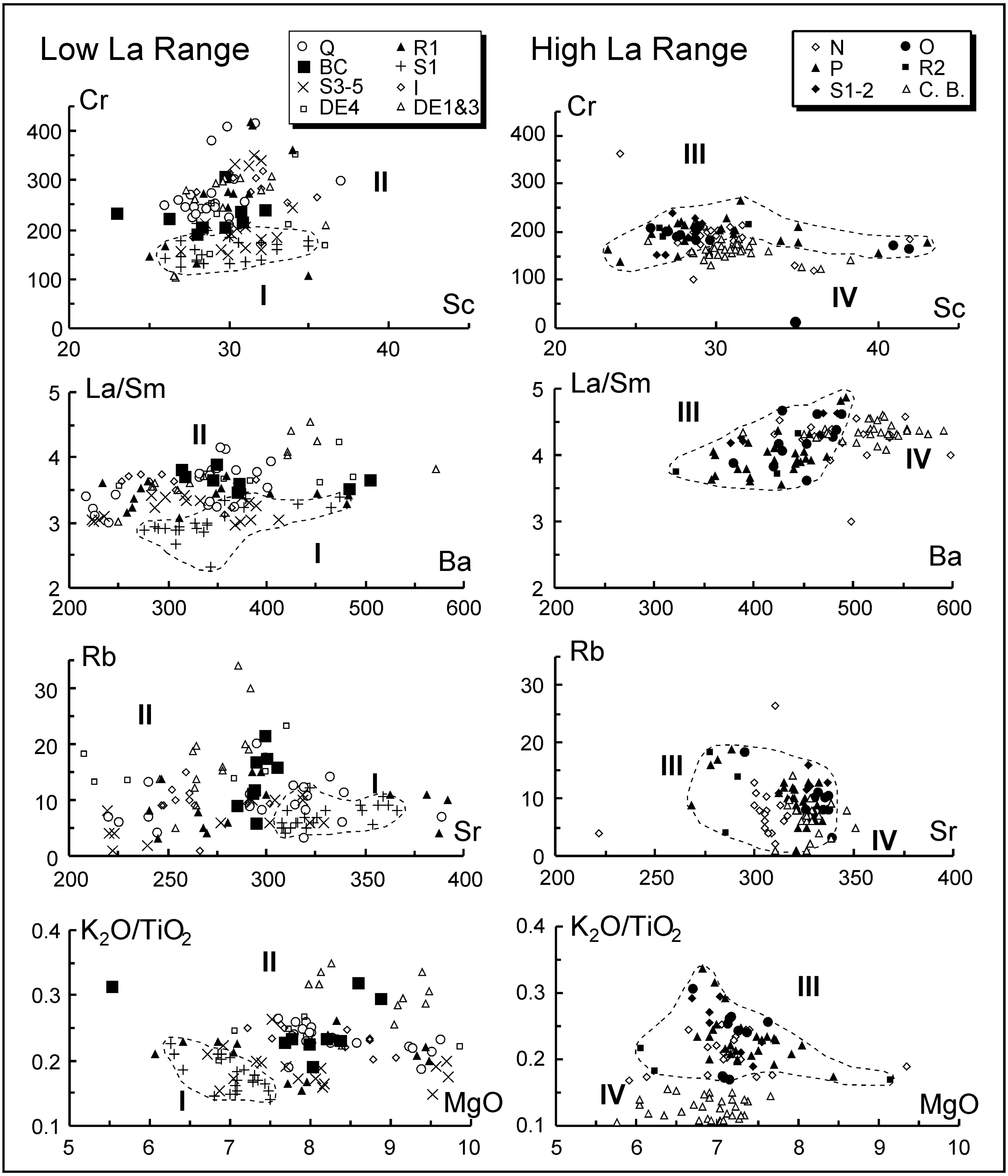

Figure 10. Variation diagrams for elements and element ratios in eastern SRP tholeiitic basalt flow groups. Each major La range is separated into two series based on geochemistry (see Figure 12). Series I and III are outlined to indicate where overlaps occur with series II and IV, respectively. See text for explanation.

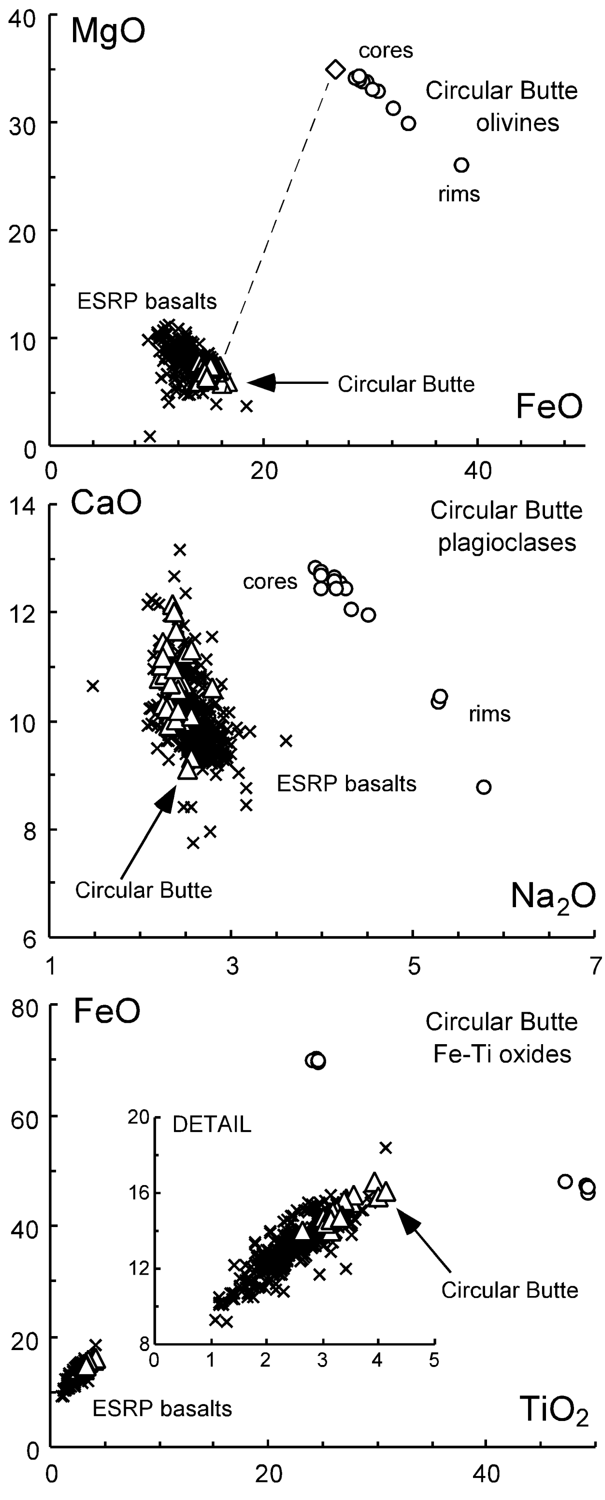

Figure 11. Electron microprobe analyses of essential mineral phases in Circular Butte lavas in the northern INEEL. Open triangles represent whole rock analyses of the Circular Butte basalts and are shown to fall within the clusters for all eastern SRP olivine tholeiites. Dashed line in top diagram connects calculated olivine composition (diamond) in equilibrium with the Circular Butte basalt.

cant trends in bulk MgO/FeO and CaO/Na_2O ratios aligned with phenocryst values. These effects are not evident in Figure 11, although the $FeO\text{-}TiO_2$ trend may be related to a small Fe-Ti oxide effect. Crystallization of olivine and plagioclase would also greatly affect compatible minor and trace elements leading to significant depletion of Sc, Cr, Ni, and Sr in the melt. Chemical variations shown in Figure 10 may be partly related to local mineralogical segregation, yet simple magmatic separation would require density differences and enough time for crystals to form and settle out or produce a mush from which liquid could be separated. Although this mechanism probably occurred on a small scale, it is unlikely responsible for more than minor geochemical changes in light of studies that imply short crustal residence times and the lack of differentiated compositions in the tholeiitic series. Crystal fractionation also does not explain the large ranges in incompatible trace elements (e.g., Shervais and others, 1994) shown by and illustrated in Figures 9 and 10. A three-fold variation in the incompatible elements, assuming a bulk distribution coefficient of zero, requires about 65-70 percent crystallization, which would result in more differentiated lithologic types than what is observed (e.g., see Shervais and others, 1994).

Vapor-differentiation may be responsible for some chemical heterogeneity in eastern SRP lavas. Vesiculation bands, 1- to 10-cm-thick layers of highly vesiculated lava, are common within the upper parts of lava inflationary lobes (Hughes and others, 1997b, 1999) and are often associated with textural variations. Massive diktytaxitic flow interiors commonly have vesicle cylinders and vesicle sheets that locally have chemically evolved compositions relative to other parts of the flow (Bates, 1999). The effect of gas exsolution on geochemical variation is potentially significant, as reported by Goff (1996) in an assessment of vapor-differentiation of diktytaxitic basalts. His results indicate that volatile-rich magmas show positive chemical correlations with lava porosity and increasing groundmass size. Vesicle cylinders and layers are enriched in many incompatible elements, as well as Fe, Mn, Ti, Na, K and P, that are not readily incorporated into minerals during the initial crystallization of the magma. Petrographic and geochemical studies of Circular Butte lavas in the northern INEEL (Casper, 1999) demonstrate that coarse diktytaxitic lavas have higher concentrations of accessory P- and REE-rich apatite and incompatible element-rich glass around irregularly shaped pore spaces.

A plot of La versus MgO for the low-La and high-La ranges (Figure 12) illustrates several important geochemical aspects of eastern SRP tholeiite evolution, most notably a general increase in La content with decreasing MgO (also noted by Shervais and others, 1994). The relatively low, wide range in MgO contents in SRP basalts (6-10 weight percent) suggest some amount of fractionation is necessary and partly responsible for the range in La. Vectors for model crystal fractionation show paths from any reasonable starting point on the diagram. Ten percent fractionation of olivine alone (X = 10 percent, OL_{100}) yields an increase of only a few ppm (parts per million) La; while 20 percent fractionation of equal amounts of olivine and plagioclase (X = 20 percent, $OL_{50}PL_{50}$) and 30 percent fractionation of pyroxene (X = 30 percent, CPX_{100}) would, respectively, produce somewhat higher variations in La. All three vectors indicate the different models expected for compatible (MgO) and incompatible (La) elements when the ratio of liquid to solid phases is high (Cox and others, 1979). Thus, the variation in La may be unrelated to, and separate from, the MgO trend,

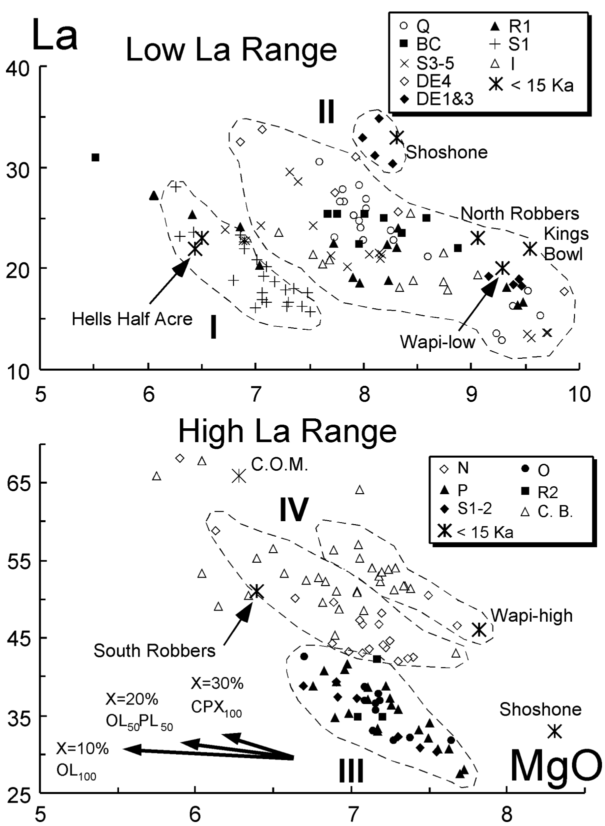

Figure 12. Variation in La (ppm) versus MgO (weight percent) for low-La (I-II) and high-La (III-V) series in eastern SRP tholeiitic basalts. Each series is represented by compositional ranges in one or more flow groups or supergroups. Except for Circular Butte (C.B.) and the <15 Ka representatives, flow group designations follow the terminology of Anderson and others (1996). Dark arrows indicate vectors for fractionation models. See text for explanation.

so olivine fractionation probably remains the most likely cause of MgO variation among SRP olivine tholeiites. This is best illustrated in the AFM diagram (Figure 5), which shows only limited departure of tholeiite compositions from the main field. The separation of a few samples from the group indicates relative increases in alkalis that may be due to crustal contamination as noted for some Yellowstone and SRP basalts (Hildreth and others, 1991).

The paucity of pyroxene as a phenocryst phase argues against significant fractionation of pyroxene, as a relatively high-pressure phase in deep crustal regimes, unless it can be shown that phenocrysts separated efficiently and the ones that did not became resorbed during magma ascent. Moreover, Cr abundances are not seriously depleted, and there are no significant positive trends in Cr versus Sc (Figure 10). One notable exception is flow group P (Figure 10) that has a range in Sc of approximately 26 to 46 ppm and may have involved a small amount of pyroxene fractionation near the source. Both elements are pyroxene compatible and would be expected to become depleted during pyroxene fractionation. Geologic evidence for this process is not apparent, but the chemical trends do not rule out pyroxene as a variable residual phase during partial melting or depletion in the source region.

Although plagioclase dominates the liquidus mineral assemblage in many SRP tholeiites, the ratio of CaO/Al_2O_3 plotted against Sc/Yb ratio in SRP basalts (Figure 13) suggests minimal involvement of plagioclase as a fractionating phase. Changes in Sc/Yb ratio may be attributed to overall increase in REE while Sc remains fairly constant. There is little change in Ca/Al except for samples collected at Circular Butte, a shield volcano consisting of coarse diktytaxitic flows that show lithologic and chemical evidence of plagioclase fractionation. Phenocryst abundances range from nearly aphyric to 30 percent; phenocryst size ranges from 2 mm to 1.5 cm, and groundmass textures range from fine to coarse. Much of this variation is evident in single flow units and, in many outcrops, little distinction can be made between phenocrystic and groundmass plagioclase (Casper, 1999).

Essentially, the La versus MgO values in Figure 12 and other covariant plots in Figure 10 illustrate the inadequacy of simple crystal fractionation to account for all the variation in trace elements (see also Shervais and others, 1994), although low pressure fractionation (less than 10 kbar) of olivine and plagioclase may be important in petrogenesis of some eastern SRP basalts (Leeman, 1982b). The high-La range diagram further implies that magmas represented by some flow groups, such as N, O, and P, are in the range where liquid to solid ratios are

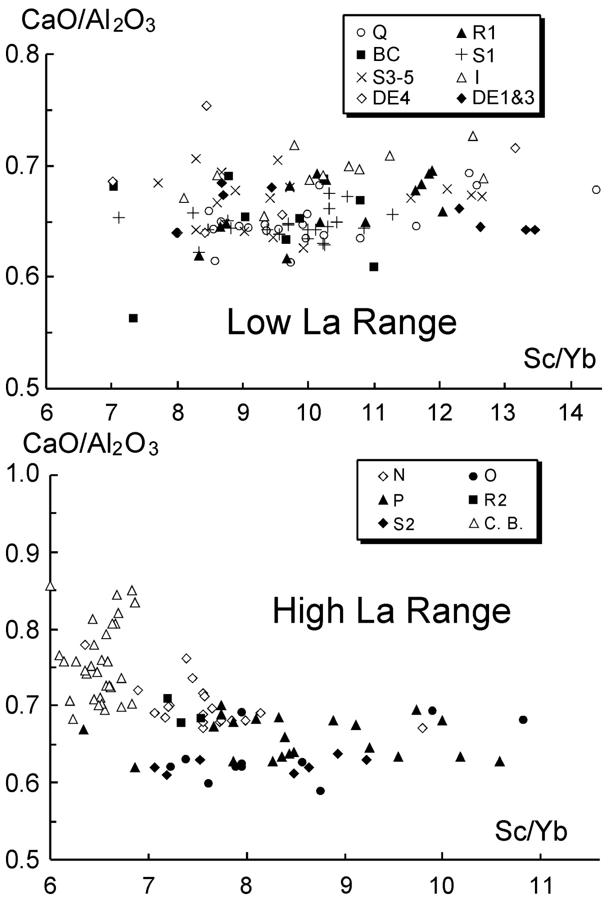

Figure 13. Covariation of CaO/Al_2O_3 ratios with Sc/Yb ratios in low La and High La range eastern SRP tholeiites. The lack of significant variation in Ca/Al ratio, with the exception of Circular Butte lavas argues against significant plagioclase fractionation. Variations in Sc/Yb reflect a large range in REE relative to Sc. See Figure 9 for explanation of flow group designations.

relatively low, such as during partial melting. Thus, the variation shown in these chemical plots supports a scenario that requires a combination of low degrees of partial melting followed by minor fractional crystallization of olivine and plagioclase.

The second major aspect of the chemical variations (Figures 10 and 12) is that several separate chemical series are evident, each of which may be represented by more than one flow group. They each have a similar trend implying similar fractionation and melting processes, albeit with different starting compositions. The late Pleistocene-Holocene examples (data from Kuntz and others, 1992) illustrate significant differences in La and MgO, and they fall along trends shown by other flow groups; however, because few trace element data are available, their individual trends cannot be observed. Separate magmatic sources are the most likely cause of producing at least four petrogenetic series (I-IV) representing two low-La and two high-La magma types. Additional series likely will be defined as more data are accumulated, especially within group II. Except for a few outlying compositions, these series are represented by flow groups using, for the time being, the terminology of Anderson and others (1996): I = S1; II = BC, DE1, DE3, DE4, I, Q, R1, and S3-5; III = O, P, R2, and S1-2; and IV = N and Circular Butte lavas in the northern INEEL.

Series II and IV are each shown as having two fields outlining apparent subseries. Little meaning can be attached to these subseries at present; however, series IV is dominated by Circular Butte lavas that represent two major flow lobes on a single monogenetic shield volcano (Casper, 1999). Also, logs of INEEL drill core show that flow group N (series IV) lies directly beneath and is conformably overlain by Circular Butte lavas, thus providing evidence for a magmatic transition with time. Considerable overlap of flow groups exists within series II and III, yet distinct trends are apparent within most flow groups attesting to their derivation from individual magma batches. Most notable are flow groups R1 and BC which have wide ranges extending to high-La, relatively low-Mg compositions.

MAGMATIC SOURCES

Chemical variations observed between SRP basalt flow group series I-IV and discrete chemical trends within individual flow groups are inconsistent with the production of a single batch of magma that differentiated by crustal assimilation and fractional crystallization. Recurrence of chemical types is apparently unrelated to spatial distribution, so the petrogenetic processes enabling each series, and probably each flow group, are randomly distributed in space and time. A source capable of producing separate batches of magma for each monogenetic shield on the eastern SRP likely would be heterogeneous, but the nature of heterogeneity is unknown. One possibility is a stratified source region (Hughes and others, 1997c) that yields melts over a range of depths and degrees of melting. Chemical variations within and between individual flow groups might be accomplished by invoking variably enriched layered subcontinental lithospheric mantle (SCLM). Each magma batch experienced a range in the amount of partial melting and fractionation.

Heterogeneous enriched subcontinental mantle apparently is important in SRP basalt genesis (e.g., Leeman and Vitaliano, 1976; Menzies and others, 1983; Reid, 1995; Hanan and others, 1997), although isotopic and chemical data suggest crustal contamination in some SRP and Yellowstone basalts (Leeman, 1982c; Hildreth and others, 1991). The covariation of Th/Yb versus Ta/Yb

(Figure 14) allows for an evaluation of source composition by greatly diminishing the effects of fractionation due to crystallization and partial melting (Pearce, 1983). Hildreth and others (1991) argue that Th/Ta enrichment in SRP basalts reflects crustal contamination (vector C); however, the trend in Figure 14 may be too broad to specify a single type of contaminant, and most samples plot within the mantle array defined by the straight boundaries. Crustal contamination of SRP tholeiites has been disregarded as a major contributor on the basis of isotopic constraints (Leeman, 1982b), although magmatic interaction with the lower crust cannot be entirely ruled out. Variations in Nd and Sr isotopic signatures with La and Sr, respectively (Figure 15, bottom), reveal no clear trend in either isotopic Nd with REE or isotopic Sr with Sr abundance. Isotopic Sr and Nd signatures (Figure 15, top) suggest an enriched EM2 type mantle (Zindler and Hart, 1986), which is characteristic of the circumcratonic domain in the western U.S. (Menzies, 1989).

The overall spread in Th/Yb and Ta/Yb (Figure 14) may be related to variable source hybridization due to a combination of subduction zone and within-plate processes (vectors S and W) that introduced components into overlying SCLM. Enrichment possibly occurred during regional Eocene calc-alkaline volcanism or Paleozoic-Mesozoic stages of lithosphere accretion. Additional heterogeneity, including source depletion and enrichment, as well as thermal weakening of lower lithosphere, possibly occurred during Miocene-Pliocene hot spot-related rhyolitic volcanism. As noted by Menzies (1989), vector S is consistent with enrichment of Proterozoic terrane by a subduction component that may have been a significant factor in subcontinental mantle evolution beneath the Snake River Plain.

A viable model of SRP tholeiitic magma generation must account for systematic increase in incompatible elements (e.g., La) during eruption as well as variability of starting compositions. Magma genesis and evolution will be evaluated in a future contribution (Hughes and others, in preparation); however, we present two hypothetical scenarios based on the previous discussion, one in which

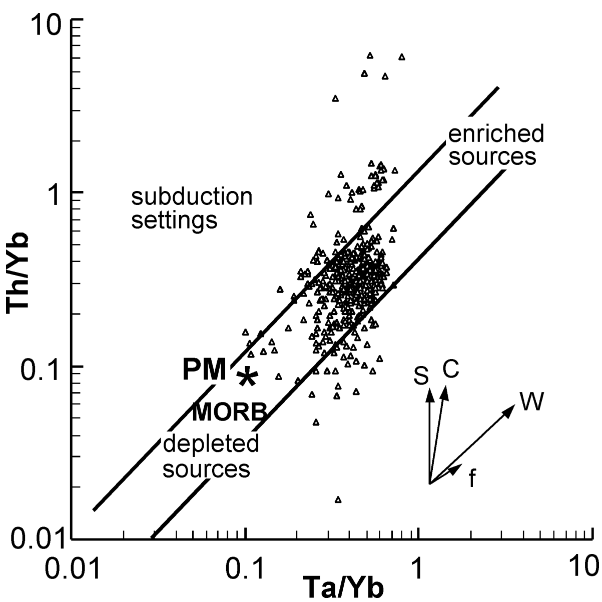

Figure 14. Th/Yb versus Ta/Yb of all eastern SRP olivine tholeiites and a few evolved compositions (see Figure 7 for data sources) showing fields of depleted mantle, enriched mantle, and mantle modified by subduction processes. Vectors represent relative contributions of modification: S—subduction zone mantle enrichment, C—crustal contamination, W—within-plate mantle enrichment, and f—fractional crystallization (after Pearce, 1983). PM—primordial mantle composition.

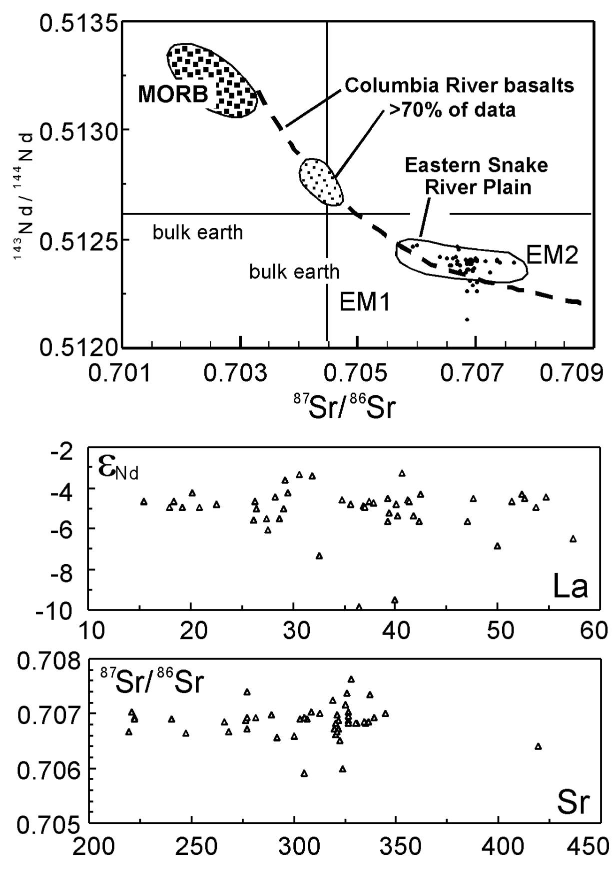

Figure 15. Isotopic Sr and Nd diagram illustrating fields of SRP olivine tholeiites, midocean ridge basalts (MORB), and the trend for Columbia River basalts (Basaltic Volcanism Study Project, 1981). New data for eastern Snake River Plain basalts (Hughes and others, 2000) are represented by small circles (top) and triangles (bottom). The bottom diagrams illustrate the lack of covariance between isotopic Nd with REE represented by La abundance and isotopic Sr with Sr abundance. Top part modified after Wilson (1989, Fig. 10.22). EM1 and EM2 mantle sources from Zindler and Hart (1986).

the chemical variation is due to partial melting and the other in which fractional crystallization is required. Primary magmas are assumed to be generated in a variably enriched, thermally weakened, SCLM source region as shown schematically in Figure 16, and they ascend without significant crustal assimilation. The models allow for variable enrichment and initial fractionation in the source region such that higher incompatible elements and less mafic bulk compositions are expected with increasing height in the SCLM. Both scenarios imply that each monogenetic shield (flow group) is derived from a separate zone of partial melting. Olivine fractionation probably occurs in all cases in order to reduce primary MgO contents below picritic levels.

Scenario 1 supposes that the melt is extracted from the center of a zone of partial melting, and the source then may or may not be tapped farther into the zone of melting where the degree of melting is progressively lower. Some magmas thus ascend with increasingly higher incompatible element abundances with depth. Variably enriched magma ascends through the ductile lower crust, opening and closing pathways plastically, and begins to fractionate olivine ± pyroxene ± plagioclase depending on depth. As the magma batch enters the brittle upper crust, it rises as a thin vertical blade along a typical rift system. Magma representing the highest degree of melting erupts first, followed by lower degree components, if any, to produce the observed time-stratigraphic increase in incompatible elements. Scenario 2 is initially similar to scenario 1, but all of the magma is assumed to be extracted into a homogeneous batch. This magma ascends to some part of the lower-middle crust where neutral bouyancy inhibits further ascent and fractionates extensively prior to continued ascent and eruption. Either successive pulses of the (monogenetic) eruption yield more chemically evolved compositions, or the magma chamber is stratified and the least-evolved tapped first.

Both scenarios present questions that require more detailed assessment. Scenario 1 does not explain the systematic increase in incompatible elements with decrease

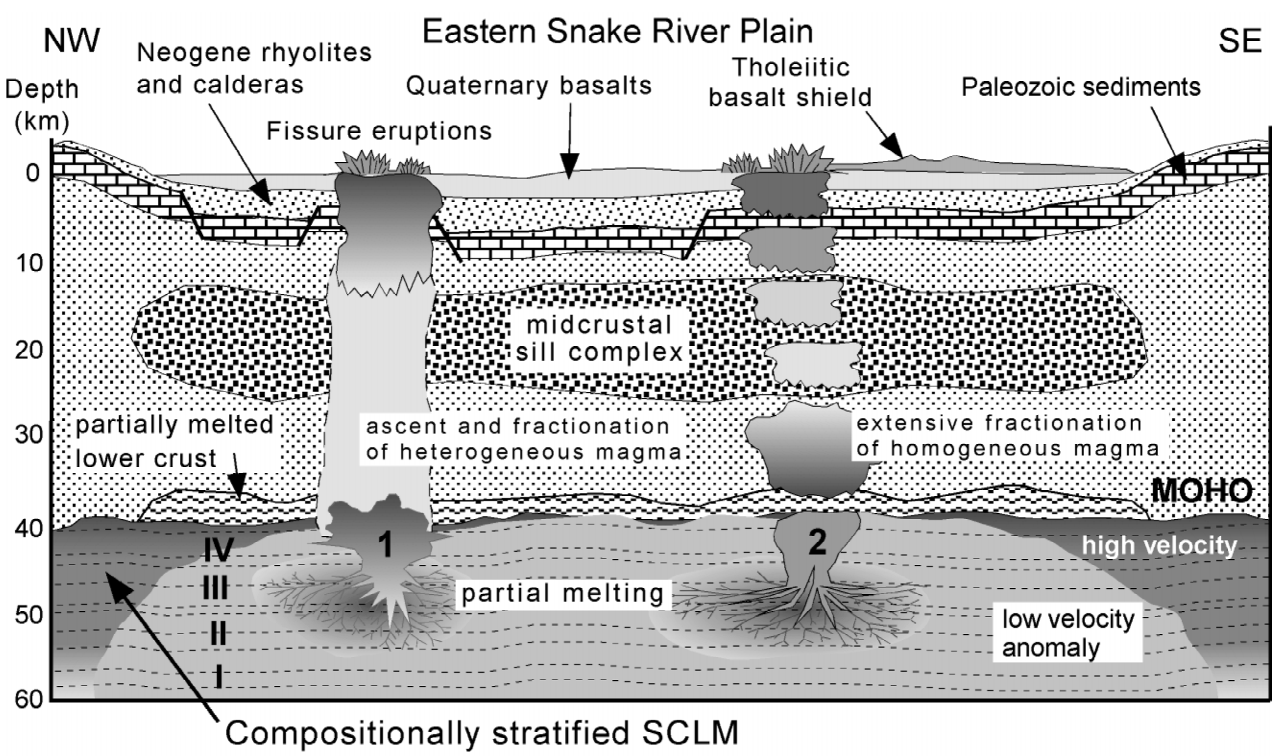

Figure 16. Schematic model of variably enriched subcontinental lithospheric mantle (SCLM) sources I-IV for basalt magma beneath the eastern SRP. View is cross-profile along the axis of the SRP (not edgewise along the rift system) illustrating broad sides of thin bladelike dike reservoirs (see Figure 4). Two hypothetical scenarios are proposed for mafic magma generation, each beginning in a restricted zone of partial melting in a compositionally stratified source region. The location of the melting zone controls the composition of the first melt, and subsequent processes are responsible for compositional diversity in a single monogenetic shield volcano. Scenario 1 requires variable degrees of partial melting followed by ascent of heterogeneous magma with minor crystal fractionation. Scenario 2 requires that a homogeneous batch of magma undergoes extensive crystal fractionation at the level of neutral bouyancy in the lower-middle crust. See text for explanation.

in MgO, unless it can be shown that MgO variability also occurs during the melting event. It also presents difficulties with magma dynamics, such that homogenization might be expected during ascent. Scenario 2 requires that the magma fractionate extensively, perhaps as much as 70 percent or more in some cases. Initial tests of fractionation models predict that any liquidus assemblage would significantly change the bulk composition to something much different than an olivine tholeiite after only 20-30 percent fractional crystallization of the most mafic SRP composition.

Regardless of what is responsible for the chemical variability, tholeiite series I and II require less enrichment than series III and IV, and series II and IV potentially represent large ranges in partial melting relative to the other series. Once a given region has experienced partial melting and magma has been extracted, further melting of the depleted residuum would be unlikely. Support for this scenario is found in chemical stratigraphy (Shervais and others, 1994; Hughes and others, 1997c, 2002) depicting overall increases in incompatible element abundances (e.g., La) with stratigraphic height in core samples, especially for older (>1 Ma) basalts in the northern INEEL region. These studies also demonstrate increases in incompatible elements with stratigraphic level in some individual flow groups as well as gross differences in geochemical signature between and within monogenetic flow groups (Figure 12). The data for Circular Butte suggest that some systems are derived from composite melting zones and yield more than one chemical series in a single volcano.

The petrologic model is consistent with seismic measurements across the eastern SRP, geophysical interpretations of crust and mantle layers, and structural interpretations of bedrock geology. Peng and Humphreys (1998) confirm the presence of an extensive 9-km thick midcrustal gabbroic sill proposed by Sparlin and others (1982). The sill was probably emplaced at approximately 10 Ma and is responsible for much of eastern SRP subsidence (McQuarrie and Rodgers, 1998). Saltzer and Humphreys (1997) indicate a corridor of low-velocity, presumably partially melted mantle extending beneath the plain to depths as great as 200 km. Peng and Humphreys (1998) suggest the low-velocity layer extends into lowermost crust, which is probably a source for more silicic SRP magmas. The model provided by Saltzer and Humphreys (1997) indicates that the low-velocity region is most likely partially melted peridotite and that melt has been extracted from surrounding regions with higher seismic velocities. They further contend that the shape of the low-velocity zone is too narrow and deep to be related to typical mantle plume geometry; thus, small-scale local convection in the upper mantle might be a more appropriate model for the dynamics of the Yellowstone hot spot. Their study demonstrates that the compositional effects of melting and melt extraction (depletion) are dominant processes within the upper mantle. This requires that the low-velocity zone, therefore, must be vertically graded with respect to mineralogy and chemical composition as depicted in Figure 16.

SUMMARY AND CONCLUSIONS

Petrologic and geochemical data suggest separate magma batches for individual shield volcanoes, each of which is represented as a flow group recognized and correlated in drill core and surface exposures. Combined major element, trace element, and isotopic Sr and Nd data support earlier studies (Leeman, 1982b; Kuntz, 1992; Kuntz and others, 1992) that eastern SRP olivine tholeiites are derived by varying degrees of partial melting in enriched subcontinental lithosphere and experience small amounts of olivine fractionation in the crust before eruption. Primary chemical variability between flow groups is caused by their derivation from multiple magmatic sources in a heterogeneous, possibly chemically stratified mantle that has been affected by prior subduction and within-plate processes. At least four broadly defined source types are proposed to account for variability in chemical signatures. Magmas ascend rapidly without significant crustal residence or chemical interaction, so they erupt as gas-charged lavas in which volatile-rich liquid segregation from coarsely crystalline diktytaxitic networks of plagioclase and olivine (and minor Fe-Ti spinel) is possible. This secondary fractionation process occurs during flow emplacement of SRP basalts, especially in zones of high volatile content (Goff, 1996; Bates, 1999).

A comparison between the locations of inferred subsurface eruptive centers and the documented volcanic rift zones (VRZ) of Kuntz and others (1992) suggests that the definition of the rift zones needs to be revised. Many inferred eruptive centers between the Arco-Big Southern Butte and Howe-East Butte VRZ are less than 5 km from the boundary of either one. This suggests that the locations of these VRZ, based upon the location of volcanic features present at the surface, are inconsistent with the location of volcanic features concealed in the subsurface. Therefore, the boundaries of these zones must be either expanded to include these subsurface eruptive centers or broken into numerous smaller, inferred rift zones or “vent corridors” as suggested by Anderson (1999). The latter option is supported by continued evaluations of geologic controls on hydraulic conductivity beneath the INEEL.

The result of either extending these VRZs to include additional eruptive centers or separating each VRZ into numerous smaller ones is that the zone in which strain is accommodated becomes more diffuse. The existence of discrete VRZs may be questioned, since extensional stress is not being mitigated within very narrow zones but rather is being distributed throughout a zone that may be as wide as 15 or 20 km. This is supported by basaltic shield dimensions and geochemical signatures suggesting magmatism characterized by low-volume batches of melt extracted from local reservoirs that are dispersed over a wide expanse of the subcontinental mantle beneath the eastern SRP. Magmatism controlled by restricted, well-defined rift systems would require structural components extending through the crust, which are not supported by seismicity in the eastern SRP. Instead, rift systems are likely placed over zones of partial melting that tend to migrate with time depending on ambient conditions and how recently melt was extracted from a previous event. Regional tectonic extension allows a diminished component of compressive stress parallel to the eastern SRP axis, thus enabling rift zones to be oriented roughly parallel to Basin and Range faults.

Spatial shifts of the focus of volcanism at and near the INEEL may have implications for the duration of local hiatuses. The INEEL has been the site of volcanic hiatuses that locally lasted anywhere from 200 k.y. to 1 m.y. Much of the southern and central INEEL has been without a volcanic event, with the exception of minor lobes from lava fields within the axial volcanic zone, since at least 200 Ka. Hiatuses such as this are not unusual for relatively small areas; however, a 200 k.y. hiatus for an area the size of the central and southern INEEL has not been demonstrated in the subsurface of that region.

ACKNOWLEDGMENTS

The authors thank all geologists who have worked to define eastern SRP basaltic systems and volcanic stratigraphy over the past two decades. We are indebted to Steve Anderson, U.S. Geological Survey, for collaborating on research to better understand stratigraphic correlations beneath the INEEL. Discussions with Mel Kuntz, U.S. Geological Survey, and David Rodgers and Mike McCurry, Idaho State University, enhanced many of the arguments presented in this paper. Technical reviews by Scott Vetter and Craig White are greatly appreciated and have significantly improved the quality of the manuscript. Much of this research was supported by grant DE-FG07-96ID13420 from the U.S. Department of Energy to the Idaho Water Resources Research Institute, subcontract KEK066-97-B to Idaho State University. Support for neutron irradiation was provided by the Radiation Center at Oregon State University, the U.S. Department of Energy Office of New Production Reactors, and Assistant Secretary for Environmental Management under DOE Idaho Operations Office Contract DE-AC07-94ID13223.

REFERENCES

Anders, E., and M. Ebihara, 1982, Solar-system abundances of the elements: Geochimica et Cosmochimica Acta, v. 46, p. 2360-2380.

Anders, M.H., J.W. Geissman, L.A. Piety, and J.T. Sullivan, 1989, Parabolic distribution of circum-eastern Snake River Plain seismicity and latest Quaternary faulting: Migratory pattern and association with the Yellowstone hot spot: Journal of Geophysical Research, v. 94, no. B2, p. 1589-1621.

Anders, M.H., and N.H. Sleep, 1992, Magmatism and extension: The thermal and mechanical effects of the Yellowstone hot spot: Journal of Geophysical Research, v. 97, p. 15,379-15,393.

Anderson, S.R., 1991, Stratigraphy of the unsaturated zone and uppermost part of the Snake River Plain aquifer at the Idaho Chemical Processing Plant and Test Reactors Area, Idaho National Engineering Laboratory, Idaho: U.S. Geological Survey Water-Resources Investigations Report 91-4058 (DOE/ID-22097), 35 p.

Anderson, S.R., D.J. Ackerman, M.J. Liszewski, and R.M. Feiburger, 1996, Stratigraphic data for wells at and near the Idaho National Engineering Laboratory, Idaho: U.S. Geological Survey Open-File Report 96-248 (DOE/ID-22127), 27 p. and 1 diskette.

Anderson, S.R., and R.C. Bartholomay, 1995, Use of natural gamma logs and cores for determining stratigraphic relations of basalt and sediment at the Radioactive Waste Management Complex, Idaho National Engineering Laboratory, Idaho: Journal of the Idaho Academy of Science, v. 31, no. 1, p. 1-10.

Anderson, S.R., and Beverly Bowers, 1995, Stratigraphy of the unsaturated zone and uppermost part of the Snake River Plain aquifer at Test Area North, Idaho National Engineering Laboratory, Idaho: U.S. Geological Survey Water-Resources Investigations Report 95-4130, (DOE/ID-22122) 47 p.

Anderson, S.R., M.A. Kuntz, and L.C. Davis, 1999, Geologic controls of hydraulic conductivity in the Snake River Plain aquifer at and near the Idaho National Engineering and Environmental Laboratory, Idaho: U.S. Geological Survey Water-Resources Investigations Report 99-4033, 38 p.

Armstrong, R.L., W.P. Leeman, and H.E. Malde, 1975, K-Ar dating, Quaternary and Neogene volcanic rocks of the Snake River Plain, Idaho: American Journal of Science, v. 275, p. 225-251.

Basaltic Volcanism Study Project, 1981, Basaltic volcanism on the terrestrial planets: New York, Pergamon Press, 1286 p.

Bates, David, 1999, The in-situ fractionation of an eastern Snake River Plain basalt flow: Implications for heterogeneous interaction with groundwater contaminants: Geological Society of America Abstracts With Programs, v. 31, no. 4, p. A-3.

Casper, J.L., 1999, The volcanic evolution of Circular Butte: Idaho State University M.S. thesis, 113 p.

Champion, D.E., M.A. Lanphere, and S.R. Anderson, 1996, Further verification and $^{40}Ar/^{39}Ar$ dating of the Big Lost River Reversed Polarity Subchron from drill core subsurface samples of the Idaho National Engineering and Environmental Laboratory, Idaho: Eos, Transactions, American Geophysical Union, 1996 fall meeting v. 77, no. 46, p. 165.

Champion, D.E., M.A. Lanphere, and M.A. Kuntz, 1988, Evidence for a new geomagnetic reversal from lava flow in Idaho: Discussion of short polarity reversal in the Brunhes and late Matuyama polarity chrons: Journal of Geophysical Research, v. 93, p. 11,667-11,680.

Cox, K.G., J.D. Bell, and R.J. Pankhurst, 1979, The Interpretation of Igneous Rocks: London, George Allen and Unwin Ltd, 450 p.

Fishel, M.L., 1993, The geology of uplifted rocks on Big Southern Butte: Implications for the stratigraphy and geochemistry of the eastern Snake River Plain: Idaho State University M.S. thesis, 178 p.

Geist, Dennis, and Mark Richards, 1993, Origin of the Columbia Plateau and Snake River Plain: Deflection of the Yellowstone plume: Geology, v. 21, p. 789-792.

Geslin, J.K., G.L. Gianniny, P.K. Link, and J.W. Riesterer, 1997, Subsurface sedimentary facies and Pleistocene stratigraphy of the northern Idaho National Engineering and Environmental Laboratory: Controls on hydrology, *in* Sunil Sharma and J.H. Hardcastle, eds., Proceedings of the 32nd Symposium on Engineering Geology and Geotechnical Engineering, p. 15-28.

Gianniny, G.L., J.K. Geslin, Jim Riesterer, P.K. Link, and G.D. Thackray, 1997, Quaternary surficial sediments near Test Area North (TAN), northeastern Snake River Plain: An actualistic guide to aquifer characterization, *in* Sunil Sharma and J.H. Hardcastle, eds., Proceedings of the 32nd Symposium on Engineering Geology and Geotechnical Engineering, p. 29-44.

Goff, Fraser, 1996, Vesicle cylinders in vapor-differentiated basalt flows: Journal of Volcanology and Geothermal Research, v. 71, p. 167-185.

Greeley, Ronald, 1977, Basaltic "plains" volcanism, *in* Ronald Greeley and J.S. King, eds., Volcanism of the Eastern Snake River Plain, Idaho: A Comparative Planetary Guidebook: National Aeronautics and Space Administration, p. 23-44.

———, 1982, The Snake River Plain, Idaho: Representative of a new category of volcanism: Journal of Geophysical Research, v. 87, p. 2705-2712.

Greeley, Ronald, and J.S. King, eds., 1977, Volcanism of the Eastern Snake River Plain, Idaho: A Comparative Planetary Guidebook: National Aeronautics and Space Administration, 308 p.

Hackett, W.R., and R.P. Smith, 1992, Quaternary volcanism, tectonics, and sedimentation in the Idaho National Engineering Laboratory area, *in* J.R. Wilson, ed., Field Guide to Geologic Excursions in Utah and Adjacent areas of Nevada, Idaho, and Wyoming: Utah Geological Survey Miscellaneous Publication 92-3, p. 1-18.

Hackett, W.R., R.P. Smith, and Soli Khericha, 2002, Volcanic hazards of the Idaho National Engineering and Environmental Laboratory, southeast Idaho, *in* Bill Bonnichsen, C.M. White, and Michael McCurry, eds., Tectonic and Magmatic Evolution of the Snake River Plain Volcanic Province: Idaho Geological Survey Bulletin 30.

Hanan, B.B., S.K. Vetter, and J.W. Shervais, 1997, Basaltic volcanism in the eastern Snake River Plain: Lead, neodymium, strontium isotope constraints from the Idaho INEL WO-2 core site basalts: Geological Society of America Abstracts with Programs, v. 29, p. A298.

Hayden, K.P., 1992, The geology and petrology of Cedar Butte, Bingham County, Idaho: Idaho State University M.S. thesis, 104 p.

Hayden, K.P., M. McCurry, W.R. Hackett, and S.A. Mertzman, 1992, Geology and petrology of Cedar Butte volcano, eastern Snake River Plain, Idaho: Geological Society of America Abstracts with Programs, v. 24, p. 6.

Hildreth, Wes, A.N. Halliday, and R.L. Christiansen, 1991, Isotopic and chemical evidence concerning the genesis and contamination of basaltic and rhyolitic magma beneath the Yellowstone Plateau volcanic field: Journal of Petrology, v. 32, p. 63-138.

Hon, K., J. Kauahihaua, R. Denlinger, and K. McKay, 1994, Emplacement and inflation of pahoehoe sheet flows: observations and measurements of active lava flows on Kilauea Volcano, Hawaii: Geological Society of America Bulletin, v. 106, p. 351-370.

Honjo, Norio, and W.P. Leeman, 1987, Origin of hybrid ferrolatite lavas from Magic Reservoir eruptive center, Snake River Plain, Idaho: Contributions to Mineralogy and Petrology, v. 96, p. 163-177.

Hughes, S.S., J.L. Casper, and D.J. Geist, 1997a, Potential influence of volcanic constructs on hydrogeology beneath Test Area North, Idaho National Engineering and Environmental Laboratory, Idaho, *in* Sunil Sharma and J.H. Hardcastle, eds., Proceedings of the 32nd Symposium on Engineering Geology and Geotechnical Engineering, p. 59-74.

Hughes, S.S., J.K. Geslin, and P.K. Link, 1998, Convoluted Quaternary volcanism and sedimentary stratigraphy of the northeastern Snake River Plain (SRP), TAN-INEEL, Idaho: Geological Society of America Abstracts With Programs, v. 30.

Hughes, S.S., and Mike McCurry, 2002, Bulk major and trace element evidence for a time-space evolution of Snake River Plain rhyolites, Idaho, *in* Bill Bonnichsen, C.M. White, and Michael McCurry, eds., Tectonic and Magmatic Evolution of the Snake River Plain Volcanic Province: Idaho Geological Survey Bulletin 30.

Hughes, S.S., M. McCurry, and D. Geist, 2002, Regional geochemical correlations and magmatic evolution of basalt flow groups at INEEL, *in* P.K. Link, L.L. Mink, and Dale Ralston, eds., Geology, Hydrogeology and Environmental Remediation, Idaho National Engineering and Environmental Laboratory, Eastern Snake River Plain: Geological Society of America Special Paper, 353, p. 151-173.

Hughes S.S., R.P. Smith, W.R. Hackett, and S.R. Anderson, 1999, Mafic volcanism and environmental geology of the eastern Snake River Plain, *in* S.S. Hughes and G.D. Thackray, eds., Guidebook to the Geology of Eastern Idaho: Idaho Museum of Natural History, p. 143-168.

Hughes, S.S., R.P. Smith, W.R. Hackett, Mike McCurry, S.R. Anderson, and G.C. Ferdock, 1997b, Bimodal magmatism, basaltic volcanic styles, tectonics, and geomorphic processes of the eastern Snake River Plain, Idaho, *in* P.K. Link and B.J. Kowallis, eds., Proterozoic to Recent Stratigraphy, Tectonics, and Volcanology, Utah, Nevada, Southern Idaho and Central Mexico: Brigham Young University Geology Studies, v. 42, Part I, p. 423-458.

Hughes, S.S., P.H. Wetmore, and J.L. Casper, 1997c, Geochemical interpretation of basalt stratigraphy and Quaternary mafic volcanism, eastern Snake River Plain, Idaho: Geological Society of America Abstracts with Programs, v. 29, p. A-298.

Knobel, L.L., L.D. Cecil, and T.R. Wood, 1995, Chemical composition of selected core samples, Idaho National Engineering Laboratory, Idaho: U. S. Geological Survey Open-File Report 95-748, 59 p.

Kuntz, M.A., 1979, Geologic map of the Juniper Buttes area, eastern Snake River Plain, Idaho: U.S. Geological Survey Miscellaneous Investigations Series, Map I-1115, scale 1:48,000.

———, 1992, A model-based perspective of basaltic volcanism, eastern Snake River Plain, Idaho, *in* P.K. Link, M.A. Kuntz, and L.P. Platt, eds., Regional Geology of Eastern Idaho and Western Wyoming: Geological Society of America Memoir 179, p. 289-304.

Kuntz, M.A., D.E. Champion, R.H. Lefebvre, and H.R. Covington, 1988, Geologic map of the Craters of the Moon, Kings Bowl, Wapi lava fields and the Great Rift volcanic rift zone, south-central Idaho: U.S. Geological Survey Miscellaneous Investigation Series Map I-1632, scale 1:100,000.

Kuntz, M.A., D.E. Champion, E.C. Spiker, and R.H. Lefebvre, 1986, Contrasting magma types and steady-state, volume-predictable volcanism along the Great Rift, Idaho: Geological Society of America Bulletin, v. 97, p. 579-594.

Kuntz, M.A., D.E. Champion, E.C. Spiker, R.H. Lefebvre, and L.A. McBroome, 1982, The Great Rift and the evolution of the Craters of the Moon lava field, Idaho, *in* Bill Bonnichsen and R.M. Breckenridge, eds., Cenozoic Geology of Idaho: Idaho Bureau of

Mines and Geology Bulletin 26, p. 423-438.

Kuntz, M.A., H.R. Covington, and L.J. Schorr, 1992, An overview of basaltic volcanism of the eastern Snake River Plain, Idaho, *in* P.K. Link, M.A. Kuntz, and L.P. Platt, eds., Regional Geology of Eastern Idaho and Western Wyoming: Geological Society of America Memoir 179, p. 227-267.

Kuntz, M.A., and G.B. Dalrymple, 1979, Geology, geochronology, and potential volcanic hazards in the Lava Ridge-Hell's Half Acre area, eastern Snake River Plain, Idaho: U.S. Geological Survey Open-File Report 79-1657, 70 p.

Kuntz, M.A., G.B. Dalrymple, D.E. Champion, and D.J. Doherty, 1980, Petrography, age, and paleomagnetism of volcanic rocks at Radioactive Waste Management Complex, Idaho National Engineering Laboratory, Idaho, with an evaluation of volcanic hazards: U.S. Geological Survey Open-File Report 80-388, 63 p.

Kuntz, M.A., N.H. Elsheimer, L.F. Espos, and P.R. Klock, 1985, Major element analyses of latest Pleistocene-Holocene lava fields of the Snake River Plain, Idaho: U.S. Geological Survey Open-File Report 85-593, 64 p.

Kuntz, M.A., Betty Skipp, M.A. Lanphere, W.E. Scott, K.L. Pierce, G.B. Dalrymple, D.E. Champion, G.F. Embree, W.R. Page, L.A. Morgan, R.P. Smith, W.R. Hackett, and D.W. Rodgers, 1994, Geologic map of the Idaho National Engineering Laboratory and adjoining areas, eastern Idaho: U.S. Geological Survey Miscellaneous Investigations Series Map 1-2330, scale 1:100,000.

Lanphere, M.A., M.A. Kuntz, and D.E. Champion, 1994, Petrography, age, and paleomagnetism of basaltic lava flows in coreholes at Test Area North (TAN), Idaho National Engineering Laboratory: U.S. Geological Survey Open-File Report 94-686, 49 p.

LaPoint, P.J.I., 1977, Preliminary photogeographic map of the eastern Snake River Plain, Idaho: U.S. Geological Survey Miscellaneous Field Studies Map MF-850, scale 1:250,000.

Le Bas, M.J., R.W. Le Maitre, A. Streckeisen, and B. Zanettin, 1986, A chemical classification of volcanic rocks based on the total alkali-silica diagram: Journal of Petrology, v. 27, p. 745-750.

Leeman, W.P., 1982a, Development of the Snake River Plain-Yellowstone Plateau Province, Idaho and Wyoming: An overview and petrologic model, *in* Bill Bonnichsen and R.M. Breckenridge, eds., Cenozoic Geology of Idaho: Idaho Bureau of Mines and Geology Bulletin 26, p. 155-177.

———, 1982b, Olivine tholeiitic basalts of the Snake River Plain, Idaho, *in* Bill Bonnichsen and R.M. Breckenridge, eds., Cenozoic Geology of Idaho: Idaho Bureau of Mines and Geology Bulletin 26, p. 181-191.

———, 1982c, Evolved and hybrid lavas from the Snake River Plain, Idaho, *in* Bill Bonnichsen and R.M. Breckenridge, eds., Cenozoic Geology of Idaho: Idaho Bureau of Mines and Geology Bulletin 26, p. 193-202.

———, 1982d, Rhyolites of the Snake River Plain-Yellowstone Plateau Province, Idaho and Wyoming: A summary of petrogenetic models, *in* Bill Bonnichsen and R.M. Breckenridge, eds., Cenozoic Geology of Idaho: Idaho Bureau of Mines and Geology Bulletin 26, p. 203-212.

Leeman, W.P., and C.J. Vitaliano, 1976, Petrology of the McKinney basalt, Snake River Plain, Idaho: Geological Society of American Bulletin, v. 87, p. 1777-1792.

Leeman, W.P., C.J. Vitaliano, and M. Prinz, 1976, Evolved lavas from the Snake River Plain, Craters of the Moon National Monument, Idaho: Contributions to Mineralogy and Petrology, v. 56, p. 35-60.

Luedke, R.G., and R.L. Smith, 1982, Map showing distribution, composition, and age of late Cenozoic volcanic centers in Oregon and Washington: U.S. Geological Survey Miscellaneous Investigations Series Map I-1091-D.

McGee, J.J., and J.W. Shervais, 1997, Flotation cumulate in a Snake River Plain ferrobasalt: Petrologic study of a possible lunar analogue: Geological Society of America Abstracts with Programs, v. 29, p. A136.

McCurry, Michael, W.R. Hackett, and Karl Hayden, 1999, Cedar Butte and cogenetic Quaternary rhyolite domes of the eastern Snake River Plain, *in* S.S. Hughes and G.D. Thackray, eds., Guidebook to the Geology of Eastern Idaho: Idaho Museum of Natural History, p. 169-179.

McQuarrie, Nadine, and D.W. Rodgers, 1998, Subsidence of a volcanic basin by flexure and lower crustal flow: The eastern Snake River Plain, Idaho: Tectonics, v. 17, no. 2, p. 203-220.

Menzies, M.A., 1989, Cratonic, circumcratonic and oceanic mantle domains beneath the western United States: Journal of Geophysical Research, v. 94, no. B6, p. 7899-7915.

Menzies, M.A., W.P. Leeman, and C.J. Hawkesworth, 1983, Isotope geochemistry of Cenozoic volcanic rocks reveals mantle heterogeneity below western USA: Nature, v. 303, p. 205-209.

———, 1984, Geochemical and isotopic evidence for the origin of continental flood basalts with particular reference to the Snake River Plain Idaho, U.S.A: Philosophical Transactions of the Royal Society of London, v. 310, p. 643-660.

Parsons, Tom, and G.A. Thompson, 1991, the role of magma overpressuring in suppressing earthquakes and topography: Worldwide examples: Science, v. 253, p. 1399-1402.

Parsons, Tom, G.A. Thompson, and R.P. Smith, 1998, More than one way to stretch: a tectonic model for extension along the plume track of the Yellowstone hot-spot and adjacent Basin and Range Province: Tectonics, v. 17, p. 221-234.

Pearce, J.A., 1983, Role of the sub-continental lithosphere in magma genesis at active continental margins, *in* C.J. Hawkesworth and M.J. Norrey, eds., Continental Basalts and Mantle Xenoliths: Cheshire, U.K., Shiva Publishing Ltd., p. 230-249.

Peng, Xiaohua, and E.D. Humphreys, 1998, Crustal velocity structure across the eastern Snake River Plain and the Yellowstone swell: Journal of Geophysical Research, v. 103, no. B4, p. 7171-7186.

Pierce, K.L., and L.A. Morgan, 1992, The track of the Yellowstone hotspot: Volcanism, faulting, and uplift, *in* P.K. Link, M.A. Kuntz, and L.P. Platt, eds., Regional Geology of Eastern Idaho and Western Wyoming: Geological Society of America Memoir 179, p. 1-53.

Pollard, D.D., P.T. Delaney, W.A. Duffield, E.T. Endo, and A.T. Okamura, 1983, Surface deformation in volcanic rift zones: Tectonophysics, v. 94, p. 541-584.

Prinz, Martin, 1970, Idaho rift system, Snake River Plain, Idaho: Geological Society of America Bulletin, v. 81, p. 941-947.

Reed, M.F., R.C. Bartholomay, and S.S. Hughes, 1997, Geochemistry and stratigraphic correlation of basalt lavas beneath the Idaho Chemical Processing Plant, Idaho National Engineering Laboratory: Environmental Geology, v. 30, p. 108-118.

Reid, M.R., 1995, Processes of mantle enrichment and magmatic differentiation in the eastern Snake River Plain: Th isotope evidence: Earth and Planetary Science Letters, v. 131, p. 239-254.

Rodgers, D.W., W.R. Hackett, and H.T. Ore, 1990, Extension of the Yellowstone Plateau, eastern Snake River Plain, and Owyhee Plateau: Geology, v. 18, p. 1138-1141.

Rubin, A.M., 1992, Dike-induced faulting and graben subsidence in volcanic rift zones: Journal of Geophysical Research, v. 97, no. B2, p. 1839-1858.

Rubin, A.M., and D.D. Pollard, 1987, Origins of blade-like dikes in volcanic rift zones: U.S. Geological Survey Professional Paper 1350, Ch. 53, p. 1449-1470.

Saltzer, R.L., and E.D. Humphreys, 1997, Upper mantle P wave velocity structure of the eastern Snake River Plain and its relationship to geodynamic models of the region: Journal of Geophysical Research, v. 102, no. B6, p. 11,829-11,841.

Scott, W.E., 1982, Surficial geologic map of the eastern Snake River Plain and adjacent areas, Idaho and Wyoming: U.S. Geological Survey Miscellaneous Investigation Map I-1372, scale 1:250,000.

Self, Stephen, Lazlo Keszthelyi, and Th. Thordarson, 1998, The importance of pahoehoe: Annual Reviews of Earth and Planetary Science, v. 26, p. 81-110.

Shervais, J.W., S.K. Vetter, and W.R. Hackett, 1994, Chemical stratigraphy of basalts in coreholes NPR-E and WO-2, Idaho National Engineering Laboratory, Idaho: Implications for plume dynamics in the Snake River Plain: Proceedings of the VIIth International Symposium on the Observation of Continental Crust Through Drilling, Santa Fe, New Mexico, p. 93-96.

Smith, R.B., and L.W. Braile, 1994, The Yellowstone hot spot: Journal of Volcanology and Geothermal Research, v. 61, p. 121-187.

Sparlin, M.A., L.W. Braile, and R.B. Smith, 1982, Crustal structure of the eastern Snake River Plain from ray trace modeling of seismic refraction data: Journal of Geophysical Research, v. 87, p. 2619-2633.

Spear, D.B., 1979, The geology and volcanic history of the Big Southern Butte-East Butte area, eastern Snake River Plain, Idaho: State University of New York at Buffalo Ph.D. dissertation, 136 p.

Stout, M.Z., and J. Nicholls, 1977, Mineralogy and petrology of Quaternary lava from the Snake River Plain, Idaho: Canadian Journal of Earth Sciences, v. 14, p. 2140-2156.

Stout, M.Z., J. Nicholls, and M.A. Kuntz, 1994, Petrological and mineralogical variations in 2500-2000 yr B.P. lava flows, Craters of the Moon lava field, Idaho: Journal of Petrology, v. 35, p. 1682-1715.

Welhan, John, Tim Funderberg, R.P. Smith, and Alan Wylie, 1997, Stochastic modeling of hydraulic conductivity in the Snake River Plain Aquifer: 1. Geologic constraints and conceptual approach, *in* Sunil Sharma and J.H. Hardcastle, eds., Proceedings of the 32nd Symposium on Engineering Geology and Geotechnical Engineering, p. 75-91.

Welhan, J.A., C.M. Johannesen, J.A. Glover, L.L. Davis, and K.S. Reeves, 2002, Overview and synthesis of lithologic controls on aquifer heterogeneity in the eastern Snake River Plain, Idaho, *in* Bill Bonnichsen, C.M. White, and Michael McCurry, eds., Tectonic and Magmatic Evolution of the Snake River Plain Volcanic Province: Idaho Geological Survey Bulletin 30.

Wetmore, P.H., 1998, An assessment of physical volcanology and tectonics of the central eastern Snake River Plain based on the correlation of subsurface basalts at and near the Idaho National Engineering and Environmental Laboratory, Idaho: Idaho State University M.S. thesis, 79 p.

Wetmore, P.H., S.S. Hughes, and S.R. Anderson, 1997, Model morphologies of subsurface Quaternary basalts as evidence for a decrease in the magnitude of basaltic magmatism at the Idaho National Engineering and Environmental Laboratory, Idaho, *in* Sunil Sharma and J.H. Hardcastle, eds., Proceedings of the 32nd Symposium on Engineering Geology and Geotechnical Engineering, p. 45-58.

Wilson, Marjorie, 1989, Igneous Petrogenesis: London, Unwin Hyman, 466 p.

Zindler, A., and S. Hart, 1986, Chemical geodynamics: Annual Reviews of Earth and Planetary Science, v. 14, p. 493-571.